AD_____

Award Number: DAMD17-01-1-0302

TITLE: STK15/BTAK and Centrosome Anomaly in Human Breast Cancer

PRINCIPAL INVESTIGATOR: Subrata Sen, Ph.D.

CONTRACTING ORGANIZATION: The University of Texas M.D. Anderson Cancer Center
Houston, Texas 77030

REPORT DATE: October 2003

TYPE OF REPORT: Final

PREPARED FOR: U.S. Army Medical Research and Materiel Command
Fort Detrick, Maryland 21702-5012

DISTRIBUTION STATEMENT: Approved for Public Release;
Distribution Unlimited

The views, opinions and/or findings contained in this report are those of the author(s) and should not be construed as an official Department of the Army position, policy or decision unless so designated by other documentation.

REPORT DOCUMENTATION PAGE

Form Approved
OMB No. 074-0188

1. AGENCY USE ONLY (Leave blank)	2. REPORT DATE	3. REPORT TYPE AND DATES COVERED
	October 2003	Final (27 Sep 2001 - 30 Sep 2003)

4. TITLE AND SUBTITLE
STK15/BTAK and Centrosome Anomaly in Human Breast Cancer

5. FUNDING NUMBERS
DAMD17-01-1-0302

6. AUTHOR(S)
Subrata Sen, Ph.D.

7. PERFORMING ORGANIZATION NAME(S) AND ADDRESS(ES)
The University of Texas M.D. Anderson Cancer Center
Houston, Texas 77030

E-Mail: ssen@mdanderson.org

8. PERFORMING ORGANIZATION REPORT NUMBER

9. SPONSORING / MONITORING AGENCY NAME(S) AND ADDRESS(ES)
U.S. Army Medical Research and Materiel Command
Fort Detrick, Maryland 21702-5012

10. SPONSORING / MONITORING AGENCY REPORT NUMBER

11. SUPPLEMENTARY NOTES

12a. DISTRIBUTION / AVAILABILITY STATEMENT
Approved for Public Release; Distribution Unlimited

12b. DISTRIBUTION CODE

13. ABSTRACT (Maximum 200 Words)

STK15/BTAk is a member of the Aurora/Ipl1 related serine/threonine kinase super family that is associated with centrsomes, exhibits elevated expression in many human cancers. Ectopic over expression of this kinase induces aneuploidy, centrosome amplification and tumorigenic transformation in cells grown in vitro. In the study conduced during this funded project, the findings are the following:

a) The familial breast cancer susceptibility gene BRCA1, which co-localizes to centrsome during mitosis, interacts with STK15 in vivo and is phosphorylated by STk15 kinase immunoprecipitated from mitotic cells in in vitro kinase assays. W have mapped the STK15 binding domain on BRCA and have mapped the putative STK15 phosphorylation site on BRCA1.
b) The tumor suppressor protein p53, which localizes to centrosome is phosphorylated by STK15 and this phosphorylation leads to destabilization and inhibition of p53.
c) The central peptide domain of STk15 isnecessary for localization of this protein kinase to the centrosomes. Centrosome localization of STK15 is augmented by sequences of both the amino and the carboxy terminal ends of the protein.

14. SUBJECT TERMS
Breast cancer

15. NUMBER OF PAGES
30

16. PRICE CODE

17. SECURITY CLASSIFICATION OF REPORT	18. SECURITY CLASSIFICATION OF THIS PAGE	19. SECURITY CLASSIFICATION OF ABSTRACT	20. LIMITATION OF ABSTRACT
Unclassified	Unclassified	Unclassified	Unlimited

Table of Contents

DAMD17-01-1-0302

Introduction:

STK15/BTAK/Aurora-A (hereafter referred to as STK15) encodes a novel serine/threonine kinase that was identified by our laboratory as a putative oncogene frequently amplified/over expressed in human breast cancer cells. Amplification and over expression of this gene has since then been reported in many other human cancers including those of colon, bladder and pancreas. STK15 kinase localizes to centrosomes and over expression of this protein coincides with centrosome amplification and chromosomal instability thus implicating this protein as a critical regulator of centrosome structure/function and chromosomal stability. In this funded project, we had proposed to:
1) Characterizing STK15 interaction with centrosomal protein centrin and
2) Investigating the peptide domain responsible for centrosomal targeting of STK15 kinase with the goal of identifying the anchoring proteins binding to the targeting peptide domain on STK15.

Body:

The research progress achieved so far on the two approved Statements of Work are described below:

Task 1:

In this task we had proposed to characterize the interaction of centrosomal protein centrin with STK15 through the cell cycle and identify the peptide domain involved in the interaction. As mentioned in my last annual report, a series of experiments failed to reveal phosphorylation of centrin by STK15 that lowered our enthusiasm to characterize this interaction further. We then decided to investigate possible interaction of STK15 with two proteins, the familial breast cancer susceptibility protein BRCA1 and the tumor suppressor protein p53, both associated with centrosomes and relevant to breast carcinogenesis. Both these proteins are key regulators of chromosomal stability and are frequently mutated or deleted in breast and ovarian cancers. It has also been shown that BRCA1 and p53 localize to centrosomes and the cells with BRCA1 and p53 null background cause centrosome amplification and chromosomal instability much like the way seen in STK15 over expressing cells.

To investigate if STK15 interacts with BRCA1 we have carried out co-immunoprecipitation experiments with anti STK15 and anti BRCA1 antibodies in exponentially growing human HeLa cells. As shown in Figure 1A, the results have revealed that STK15 interacts with BRCA1. The binding domain of BRCA1 has been mapped with GST pull down assay as spanning the amino acid residues 1314 and 1863 in the amino terminal end of the protein (Figure 1B).

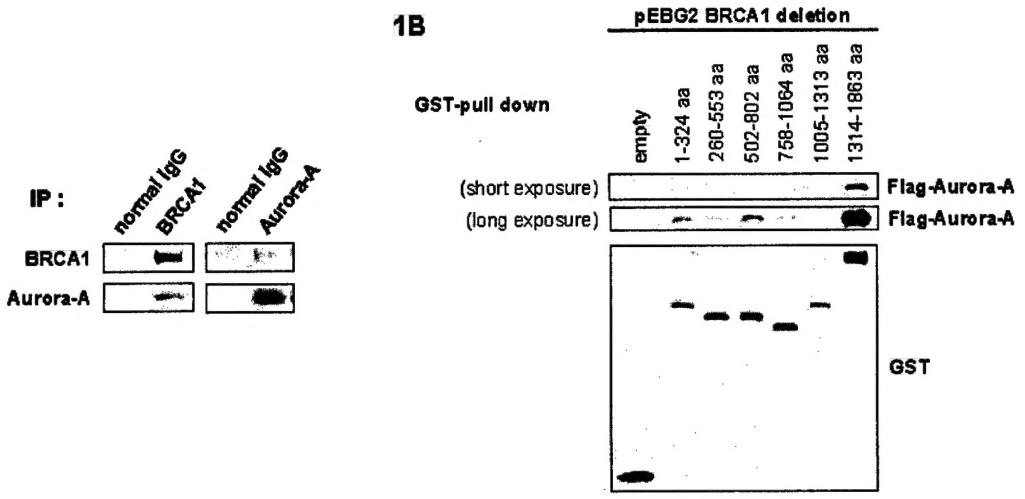

Figure 1. (A) Co immunoprecipitation experiments demonstrating in vivo interaction between STK15 and BRCA1. (B) GST pull down assay showing the BRCA1 binding domain

To examine whether or not BRCA1 is one of the substrates of STK15, we have performed in vitro kinase assay using mitotic active STK15 kinase and T7 tagged BRCA1 as substrate. A clear phosphorylation signal was detected on BRCA1, thus documenting that BRCA1 is a natural substrate of STK15 kinase. Next, we have made a series of deletions constructs of BRCA1 to determine the phosphorylation site on BRCA1. These experiments have suggested that the peptide domain between amino acid residues 758 and 1064 of the BRCA1 protein is phosphorylated by STK15 kinase. Further mapping of the phosphorylation site has narrowed down the putative phosphorylated residue to four serine residues within the peptide (Figure 2A and 2B). It is relevant to mention that this domain is encoded within the exon 11 of the BRCA1 gene, which has been shown to play a critical role in maintaining chromosomal stability and centrosomal organization. Functional significance of STK15 phosphorylation of this peptide domain is being currently investigated.

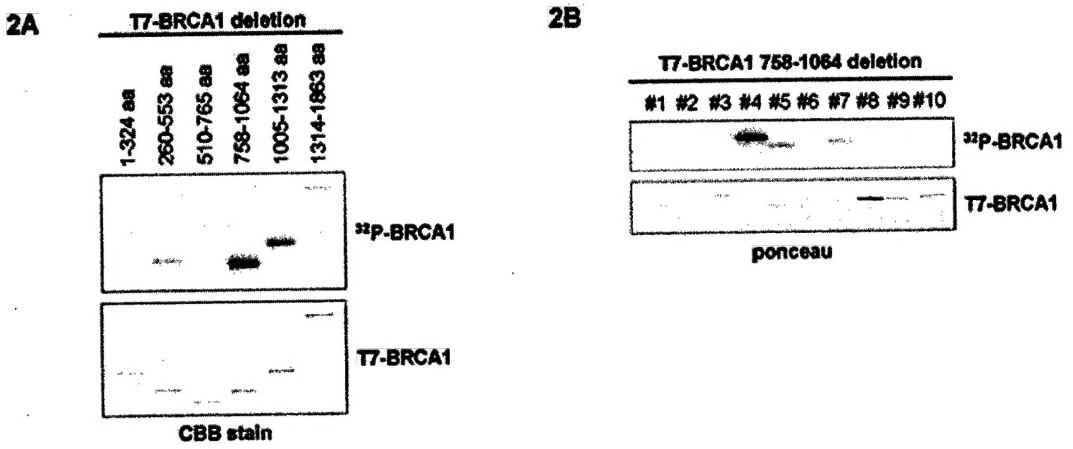

Figure 2 (A). In vitro kinase assay of different BRCA1 deletion constructs in presence of STK15 kinase. (B). In vitro kinase assay of deletion constructs of BRCA1 (758-1064) peptide in presence of STK15 kinase.

In another study, we have identified p53 as a substrate of STK15 kinase. We have also demonstrated that STK15 kinase phosphorylates p53 on Ser315 and this phosphorylation leads to Mdm2 mediated destabilization and inhibition of p53. A paper describing these findings is in press as an article to be published in ***Nature Genetics*** (Preprint attached).

Task 2:

In this task, we had proposed to identify the STK15 peptide domain necessary for targeting STK15 kinase to the centrosomes and for possible recruitment of other centrosomal proteins. The strategy involved making deletion and site directed mutants of STK15 to identify the peptide domains necessary for these functions. We have pursued this study through examination of a functional GFP-STK15 fusion protein in transient and stably (tet-regulated) transfected cells (both fixed and live), and assaying the structural dynamics of STK15 association with both the centrosome and spindle. Time-lapse microscopy of living cells demonstrates that centrosome pairs are motile throughout interphase and undergo a tumbling motion that requires intact microtubules and ATP. To establish the relationship of GFP-STK15 to centrosome and spindle architecture, cells were detergent-extracted prior to fixation, and followed by real-time monitoring of live cells during extraction. Quantitative analysis of interphase cells reveals that most (~90%) of the STK15 is detergent soluble while STK15 labeling of extensively extracted mitotic cells retains a microtubule-like distribution. A photobleaching approach was employed to compare the relative mobility of centrosome-associated GFP-STK15, GFP-β-tubulin, GFP-γ-tubulin and GFP-NuMA. Results show GFP-STK15 moves rapidly in and out of the centrosome and metaphase spindle with recovery

half-lives on the order of seconds (~3 sec) establishing its marked molecular interactions with these cellular structures. In contrast, ά-and γ-tubulin are relatively immobile, with no appreciable recovery for ~1 minute indicative of their structural role in the centrosome and spindle. NuMA protein exhibits intermediate mobility in both the interphase nucleus and at the mitotic spindle. The rapid recovery of STK15 at the centrosome is unaffected by microtubule disruption and ATP depletion. Mutational analyses indicate that a central domain of STK15 is required for centrosomal localization that is augmented by both the amino and carboxy terminal ends of the protein. Collectively, these studies contrast the relative cellular and molecular dynamics of STK15 with other cytoskeletal proteins that share its micro-domain around the MTOC and spindle, and identify essential domains required for targeting and dynamics. The finding of greater molecular mobility of STK15 over tubulin favors a more dynamic relationship of the kinase along microtubules and supports a regulatory role in spindle dynamics and chromosome movement. The results of these studies have been presented at the Era of Hope Department of Defense Breast Cancer Research Program meeting held in Orlando, Florida in September 2002 and have since then also been published.

Key Research Accomplishments:

1. STK15 interacts with and phosphorylates the familial breast cancer susceptibility gene BRCA1 that is also localized on centrosomes during mitosis like STK15. (Please treat this unpublished information as **Privileged** and **Confidential** at this time).
2. STK15 interacts and phosphorylates the tumor suppressor protein p53 and this phosphorylation destabilizes and inhibits p53.
3. A central peptide domain on STK15 is essential for its localization on centrosomes that is augmented by both the amino and the carboxy terminal ends of the protein.
4. STK15 is rapidly exchanged in and out of the centrosomes and mitotic spindle ($t_{1/2}$~3 seconds) in contrast to the ά-and γ-tubulins that are relatively immobile indicative of a structural role.

Reportable Outcomes:

Abstract:

1.Sen S., Zhou H., Mancini M., Brinkley B.R. Centrosomal targeting and dynamics of tumor amplified STK15/BTAK/Aurora-A kinase. P42-9. Era of Hope Department of Defense Breast Cancer Research Program Meeting, Orlando, Florida, 2002.

Publication:

2.Stenoien D.L., **Sen S.**, Mancini M.A., Brinkley B.R. Dynamic association of a tumor amplified kinase, Aurora-A with centrosome and mitotic spindle. ***Cell Motility & Cytoskeleton*, 55: 134-146, 2003.**

3. Katayama, H., Sasai, K., Kawai, H., Yuan, Z-M., Bondaruk, J., Suzuki, F., Fujii, S., Arlinghaus, R.B., Czerniak, B., **Sen, S..**, Phosphorylation by aurora kinase A induces Mdm2 mediated destabilization and inhibition of p53. ***Nature Genetics.*** **(In Press).**

Appendices:

Abstract:

1.Sen S., Zhou H., Mancini M., Brinkley B.R. Centrosomal targeting and dynamics of tumor amplified STK15/BTAK/Aurora-A kinase. P42-9. Era of Hope Department of Defense Breast Cancer Research Program Meeting, Orlando, Florida, 2002.

Publication:

2.Stenoien D.L., **Sen S.**, Mancini M.A., Brinkley B.R. Dynamic association of a tumor amplified kinase, Aurora-A with centrosome and mitotic spindle. ***Cell Motility & Cytoskeleton*** **, 55: 134-146, 2003.**

3. Katayama, H., Sasai, K., Kawai, H., Yuan, Z-M., Bondaruk, J., Suzuki, F., Fujii, S., Arlinghaus, R.B., Czerniak, B., **Sen, S..**, Phosphorylation by aurora kinase A induces Mdm2 mediated destabilization and inhibition of p53. ***Nature Genetics.*** **(In Press).**

CENTROSOMAL TARGETING AND DYNAMICS OF TUMOR-AMPLIFIED STK15/BTAK/AURORA A KINASE

Subrata Sen, Hongyi Zhou, Michael M. Mancini, and Bill R. Brinkley

The University of Texas M.D. Anderson Cancer Center, Baylor College of Medicine, Houston, TX 77030

ssen@mail.mdanderson.org

The STK15/BTAK/Aurora A kinase is a member of the Aurora/Ipl-1 related serine/threonine kinase super family that is associated with centrosomes, exhibits increased expression in several human tumors and induces aneuploidy when over expressed in mammalian cells. Aurora A is located at the interphase centrosomes and mitotic spindle and over expression leads to amplification of centrosome number. We have used a functional GFP- Aurora A fusion protein in transfected cells to study the sequence requirements for centrosome targeting of the kinase and also the dynamics of Aurora a association with centrosomes.

Mutational analyses indicate that kinase activity is not required but a carboxy terminal domain of Aurora A is required for centrosomal localization.

Fluorescence recovery after photobleaching (FRAP) was employed to investigate the mobility of GFP-Aurora A during interphase and mitosis. Results show that GFP-Aurora A shuttle back and forth rapidly from the centrosome and mitotic spindle with recovery half lives on the order of seconds. Partial deletion of the carboxy terminus causes significantly slower dynamics of the Aurora A photobleach recovery. These studies identify the essential domains required for targeting and dynamics of Aurora A kinase to the centrosomes and suggests a regulatory role of this kinase in centrosome function.

Studies are currently underway to identify the proteins interacting with the Aurora A kinase domains involved in its targeting and dynamic recovery to the centrosomes.

The U.S. Army Medical Research and Materiel Command under DAMD17-01-1-0302 supported this work.

nature genetics

Phosphorylation by aurora kinase A induces Mdm2-mediated destabilization and inhibition of p53

Hiroshi Katayama[1], Kaori Sasai[1], Hidehiko Kawai[2,3], Zhi-Min Yuan[2], Jolanta Bondaruk[4], Fumio Suzuki[3], Satoshi Fujii[1], Ralph B Arlinghaus[1], Bogdan A Czerniak[4] & Subrata Sen[1]

Aurora kinase A (also called STK15 and BTAK) is overexpressed in many human cancers. Ectopic overexpression of aurora kinase A in mammalian cells induces centrosome amplification, chromosome instability and oncogenic transformation, a phenotype characteristic of loss-of-function mutations of p53. Here we show that aurora kinase A phosphorylates p53 at Ser315, leading to its ubiquitination by Mdm2 and proteolysis. p53 is not degraded in the presence of inactive aurora kinase A or ubiquitination-defective Mdm2. Destabilization of p53 by aurora kinase A is abrogated in the presence of mutant Mdm2 that is unable to bind p53 and after repression of Mdm2 by RNA interference. Silencing of aurora kinase A results in less phosphorylation of p53 at Ser315, greater stability of p53 and cell-cycle arrest at G2-M. Cells depleted of aurora kinase A are more sensitive to cisplatin-induced apoptosis, and elevated expression of aurora kinase A abolishes this response. In a sample of bladder tumors with wild-type p53, elevated expression of aurora kinase A was correlated with low p53 concentration. We conclude that aurora kinase A is a key regulatory component of the p53 pathway and that overexpression of aurora kinase A leads to increased degradation of p53, causing downregulation of checkpoint-response pathways and facilitating oncogenic transformation of cells.

Aurora kinase A is a member of a new family of serine/threonine kinases that includes *Drosophila melanogaster* Aurora and *Saccharomyces cerevisiae* Ipl1 kinase, both of which are essential for controlling normal chromosome segregation and centrosome functions[1–3]. Aurora kinase A has been implicated in regulating centrosome function, spindle assembly, spindle maintenance and mitotic commitment in cells[4–7]. *AURKA*, encoding aurora kinase A, is a putative oncogene that is amplified and overexpressed in many human cancers[8–13]. The molecular targets of aurora kinase A have not been well characterized. We previously reported that phosphorylation-mediated feedback between aurora kinase A and protein phosphatase 1 operates through mitosis and that disruption of this interaction results in defects in chromosome segregation[14].

Overexpression of aurora kinase A[8] and loss of wild-type p53 function induce similar phenotypes of centrosome amplification and aneuploidy in cells[15,16]. These observations suggest that gain of aurora kinase A function and loss of wild-type p53 function may be interdependent in common pathways. The finding that human tumors with elevated expression of aurora kinase A have wild-type *TRP53* (encoding p53) also suggests that gain of aurora kinase A function may cause loss of wild-type p53 function, contributing to malignant transformation.

p53 induces growth arrest or apoptosis in cells exposed to stress and is frequently mutated or deleted in human cancers. Expression of p53 is controlled by Mdm2, which promotes ubiquitination by E3 ubiquitin ligase activity and degradation of p53 by the cytoplasmic 26S proteasome[17]. Stability and activity of p53 are also regulated by post-translational modifications[18–23] including phosphorylation, acetylation, glycosylation and attachment of a small ubiquitin-related modifier protein. Phosphorylation at multiple sites is the predominant mechanism known to stabilize and abrogate Mdm2-mediated ubiquitination and activates p53. In contrast, phosphorylation of the core domain at Thr155 by the COP9 signalosome has been reported to target p53 for degradation[24]. The present study investigated whether phosphorylation by aurora kinase A also regulates p53 activity.

RESULTS

Aurora kinase A phosphorylates and interacts with p53

We first investigated the ability of aurora kinase A to phosphorylate p53 in an *in vitro* kinase assay. We incubated bacterially expressed glutathione S-transferase (GST) and a GST-p53 fusion protein with aurora kinase A immunoprecipitated from mitotic HeLa cells and γ^{32}P ATP. The aurora kinase A immunocomplex clearly phosphorylated GST-p53 (**Fig. 1a**). To confirm the specificity of aurora kinase A in phosphorylating p53, we used immunoprecipitated wild-type and kinase-inactive aurora kinase A (K162R) in an *in vitro* kinase assay with GST-p53. Wild-type aurora kinase A phosphorylated p53 but the kinase-inactive mutant did not (**Fig. 1b**), confirming that aurora

[1]Department of Molecular Pathology, Division of Pathology & Laboratory Medicine, University of Texas M.D. Anderson Cancer Center, Houston, Texas 77030, USA. [2]Department of Cancer Cell Biology, Harvard School of Public Health, Boston, Massachusetts 02115, USA. [3]Department of Molecular Radiobiology, Research Institute for Radiation Biology and Medicine, Hiroshima University, Hiroshima 734-8553, Japan. [4]Department of Pathology, Division of Pathology & Laboratory Medicine, University of Texas M.D. Anderson Cancer Center, Houston, Texas 77030, USA.Correspondence should be addressed to S.S. (ssen@mail.mdanderson.org).

Published online 14 December 2003; doi:10.1038/ng1279

kinase A specifically phosphorylates p53 *in vitro*. We examined the pattern of phosphorylation of p53 by aurora kinase A *in vitro* by phosphorylated-amino-acid and two-dimensional phosphopetide analysis of ^{32}P-labeled GST-p53 after digestion with N-tosyl-L-phenylalanine-chloromethyl ketone–trypsin[25]. We detected radioactive signal at the phosphoserine marker, indicating that aurora kinase A phosphorylates p53 at a serine residue (**Fig. 1c**). Two-dimensional phosphopeptide analysis showed a phosphorylated peptide in the second dimension (**Fig. 1d**). Edman degradation[26] showed that the highest radioactivity was released after the ninth cycle (**Fig. 1e**), corresponding to the serine at position 315 of p53. An *in vitro* kinase assay using GST-p53 showed that wild-type p53, but not S315A mutant p53, was phosphorylated by aurora kinase A (**Fig. 1f**).

To investigate phosphorylation of Ser315 by aurora kinase A *in vivo*, we expressed wild-type and S315A mutant p53 with either constitutively activated (T288D) or kinase-inactive mutants of aurora kinase A in HEK293 cells. We detected a strong signal with an antibody to p53 phosphorylated at Ser315 in cells expressing the constitutively activated aurora kinase A and weaker signals in the cells expressing the kinase-inactive control, probably due to endogenous aurora kinase A in these cells. We detected no signal in cells expressing S315A mutant p53, confirming that aurora kinase A phosphorylates p53 at Ser315 *in vivo* (**Fig. 1g**).

To determine whether the interaction between aurora kinase A and p53 occurs *in vitro*, we incubated ^{35}S-labeled *in vitro*–translated p53 constructs expressing either GST-tagged full-length aurora kinase A or

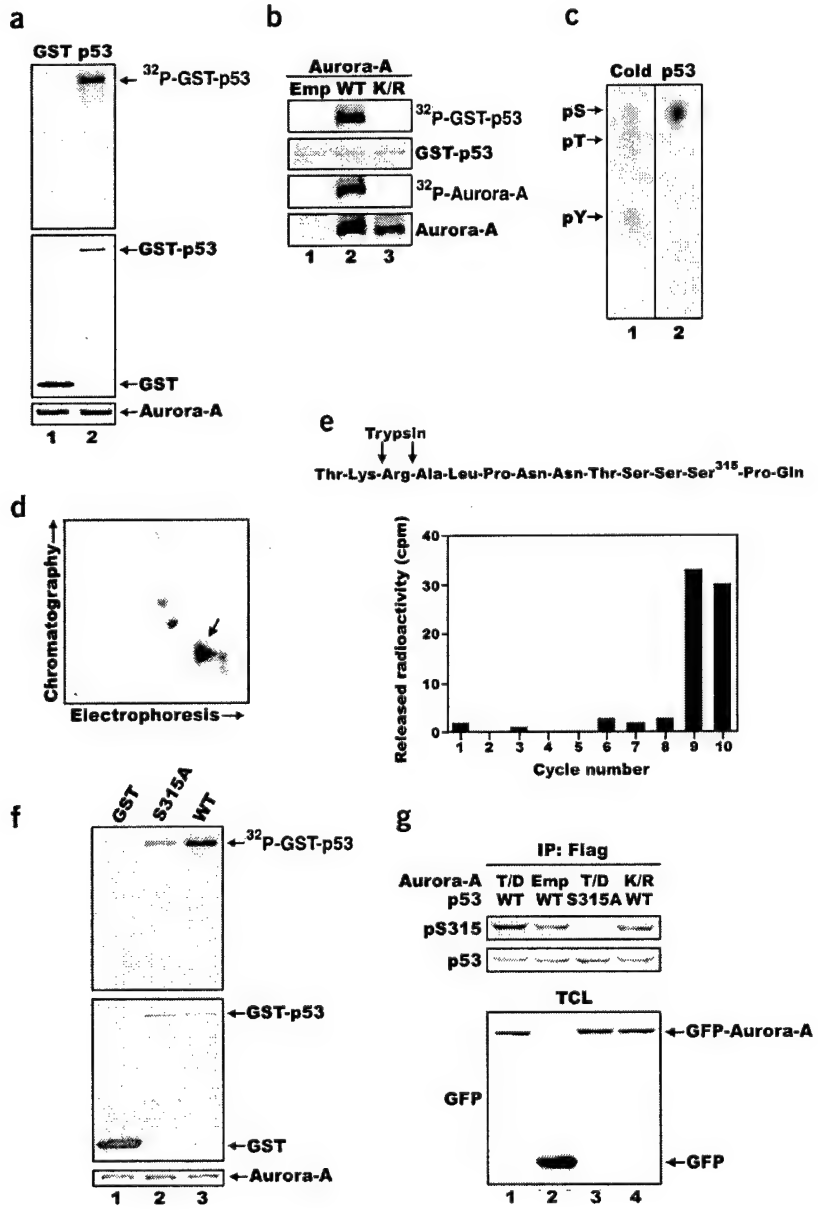

Figure 1 Aurora kinase A phosphorylates p53 at Ser315. (**a**) Immunoprecipitates with antibody to aurora kinase A from nocodazole-treated mitotic HeLa cells were incubated with either GST (lane 1) or GST-p53 (lane 2) in the presence of [γ^{32}P]ATP. GST proteins were resolved by SDS-PAGE and visualized by autoradiography (for kinase assay, top) or Coomassie blue staining (middle). Immunoprecipitates were detected with antibody to aurora kinase A (bottom). (**b**) Immunoprecipitates with antibody to Flag M2 from nocodazole-treated mitotic HeLa cells transfected with empty vector (Emp; lane 1), Flag–wild-type aurora kinase A (WT; lane 2) or Flag–aurora kinase A K162R (lane 3) were incubated with GST-p53 in the presence of [γ^{32}P]ATP. GST-p53 was resolved and visualized as in **a** (first and second rows). Immunoprecipitates were immunoblotted with antibody to Flag M2 (fourth row). Autophosphorylation of Flag–aurora kinase A was visualized by autoradiography (third row). (**c**) Trypsin-digested and HCl-treated ^{32}P-labeled GST-p53 purified by SDS-PAGE was resolved by thin layer chromatography together with phosphorylated amino acid marker. Cold indicates the position of phosphorylated amino acid markers (pS, phosphoserine; pT, phosphothreonine; pY, phosphotyrosine). (**d**) Trypsin-digested ^{32}P-labeled peptides as in **c** were subjected to two-dimensional phosphopeptide mapping. Arrow indicates the major phosphopeptide. (**e**) Amino acid sequence including and surrounding Ser315 showing N-terminal trypsin cleavage sites (top). Phosphopeptide indicated by arrow was extracted from the thin-layer-chromatography plate and subjected to Edman degradation. Released radioactivity was monitored at each cycle (shown as bar graphs). (**f**) GST, GST–p53 S315A and GST–wild-type p53 (WT) were incubated with aurora kinase A immunoprecipitates and [γ^{32}P]ATP as in **a**. Proteins were resolved and visualized as in **a**. (**g**) Flag–wild-type p53 (WT; lanes 1, 2 and 4) or Flag–p53 S315A (lane 3) were cotransfected with GFP–aurora kinase A T288D (T/D; lanes 1 and 3), GFP-empty vector (Emp; lane 2) or GFP–aurora kinase A K162R (K/R; lane 4) into HEK293 cells. Twenty-four hours after transfection, p53 was immunoprecipitated (IP) with antibody to Flag M2 and immunoprecipitates were immunoblotted with antibody to p53 phosphorylated at Ser315 and antibody to p53 (top and middle). Aliquots of the same total cell lysate (TCL) were directly immunoblotted with antibody to GFP (bottom).

the control GST alone. Aurora kinase A showed specific binding to p53 (**Fig. 2a**). We also carried out a reverse experiment in which we incubated GST-tagged p53 constructs representing the N-terminal domain (amino acids 1–112), the central DNA binding domain (amino acids 93–290) and the C-terminal domain (amino acids 291–393) with ^{35}S-labeled *in vitro*–translated full-length aurora kinase A. Aurora kinase A bound to the C-terminal domain of p53 (residues 291–393; **Fig. 2b**). To map the aurora kinase A domains involved in this interaction, we tested the *in vitro* binding of GST-tagged deletion constructs of aurora kinase A with ^{35}S-labeled *in vitro*–translated full-length p53. The C-terminal end of aurora kinase A (residues 312–403) showed no binding, but the rest of the aurora kinase A peptide, including the N-terminal end, did bind p53 (**Supplementary Fig. 1** online). The aurora kinase A box, contrary to a previous report[27], was not essential for this interaction.

We verified *in vivo* binding of endogenous aurora kinase A and p53 in Cos1 cells by coimmunoprecipitation and immunoblotting experiments (**Fig. 2c**). We verified the specificity of this coimmunoprecipitation in p53-deficient Saos-2 cells, in which aurora kinase A did not precipitate with antibody to p53 (**Supplementary Fig. 1** online). Coimmunoprecipitation experiments in MCF7 and HEK293 cells with wild-type p53 and in SW480 cells with mutant p53 (R273H) showed that aurora kinase A interacts with both wild-type and mutant p53 under physiological conditions in human cells (**Fig. 2d**). We evaluated the role of conformational changes to p53 in influencing the interaction between p53 and aurora kinase A *in vivo* in human cells with different p53 mutants. Coimmunoprecipitation experiments showed that p53 conformational mutants R175H and R249S had substantially less or no interaction with aurora kinase A (**Supplementary Fig. 1** online), suggesting that conformation rather than functional inactivation is important for interaction of p53 with aurora kinase A. We carried out *in vivo* binding assays in p53-deficient H1299 cells cotransfected with wild-type or kinase-inactive aurora kinase A together with wild-type or S315A mutant p53. These assays showed that p53 could interact with both the wild-type and kinase-inactive forms of aurora kinase A with equal efficiency and that this interaction was not influenced by phosphorylation of p53 at Ser315 (**Fig. 2e**).

In vivo phosphorylation of p53 at Ser315 was previously mapped, but the biological relevance of this modification is controversial. Phosphorylation of p53 at Ser315 both enhances sequence-specific DNA-binding activity *in vitro*[28] and reverses the stabilizing and activating effects of Ser392 phosphorylation on tetramer formation[29]. Because p53-mediated regulation of checkpoint response is activated when p53 is stabilized at both G1-S and G2-M transitions of the cell cycle[30], we investigated whether interaction between p53 and aurora kinase A and phosphorylation of p53 at Ser315 also varies in a cell cycle–dependent manner. In U2-OS cells, with wild-type p53, the steady-state level of aurora kinase A progressively increased from G1-S

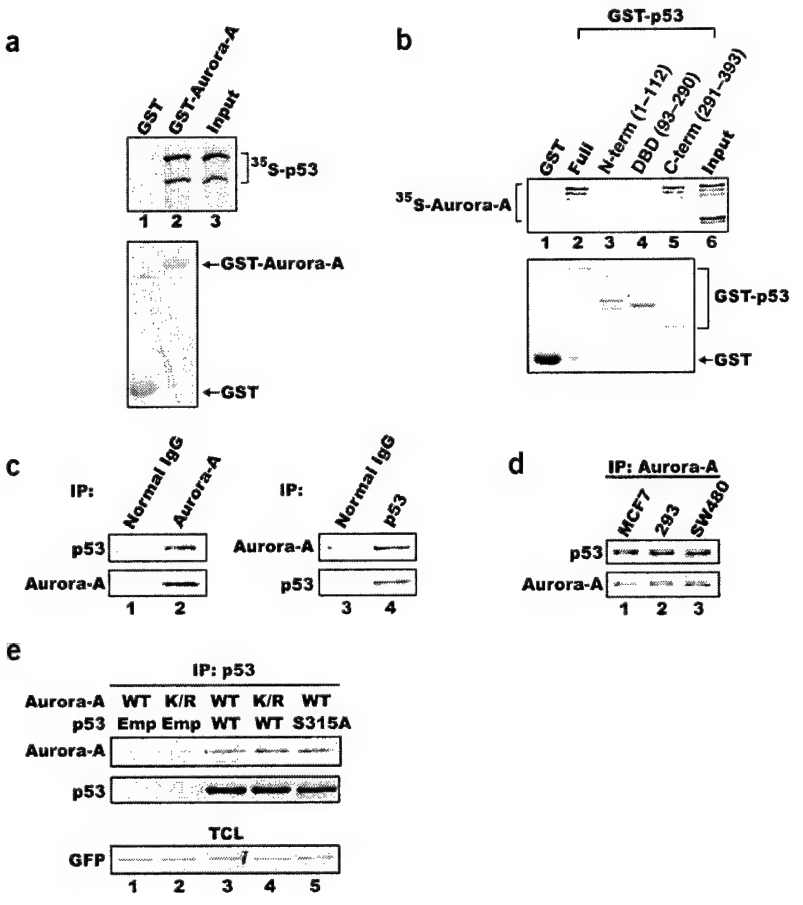

Figure 2 Aurora kinase A interacts with p53. **(a)** ^{35}S-labeled, *in vitro*–translated p53 was incubated with the beads bound either with GST or with GST–aurora kinase A. After binding, the beads were resolved by SDS-PAGE and visualized by autoradiography (for binding, top) or Coomassie blue staining (bottom). **(b)** ^{35}S-labeled, *in vitro*–translated aurora kinase A was incubated with the beads bound with GST, with GST–full length p53 (Full) or with a series of GST-p53 partial peptides (N-terminal (N-term), amino acids 1–112; DBD (DNA binding domain), amino acids 93–290; C-terminal (C-term), amino acids 291–393) followed by analysis as in **a**. **(c)** Cos1 cells were immunoprecipitated (IP) with normal IgG (lane 1) or with antibody to aurora kinase A (lane 2). Immunoprecipitates were immunoblotted with antibody to p53 and antibody to aurora kinase A (left). Right panel shows reciprocal experiment. Immunoprecipitates with normal IgG (lane 3) or with antibody to p53 (lane 4) were immunoblotted with antibody to aurora kinase A and antibody to p53. **(d)** MCF7 (lane 1), 293 (lane 2) and SW480 (lane 3) cells were immunoprecipitated (IP) with antibody to aurora kinase A and immunoprecipitates were immunoblotted with indicated antibodies. **(e)** H1299 cells were either transfected with GFP–wild-type aurora kinase A (WT; lane 1), with GFP–aurora kinase A K162R (K/R; lane 2) or with GFP–wild-type aurora kinase A and wild-type p53 (lane 3), with GFP–aurora kinase A K162R and wild-type p53 (lane 4) or with GFP–wild-type aurora kinase A and p53 S315A (lane 5). Twenty-four hours after transfection, p53 was immunoprecipitated with antibody to p53 and immunoprecipitates were immunoblotted with indicated antibodies (top and middle). Aliquots of the same total cell lysates (TCL) were directly immunoblotted with antibody to GFP (bottom). Emp, empty vector.

through G2-M phase, whereas the level of p53-bound aurora kinase A was comparable throughout the cell cycle. p53 phosphorylated at Ser315 was detectable throughout the cell cycle, but the relative amount of this species increased in S phase and during G2-M phase (**Supplementary Fig. 2** online).

Phosphorylation by aurora kinase A destabilizes p53

Because gain of function of aurora kinase A through overexpression gives rise to cellular phenotypes similar to those seen with loss of function of p53, we hypothesized that phosphorylation of p53 at Ser315 by aurora kinase A inactivates p53 by enhancing its proteolytic degradation. To address the issue, we cotransfected H1299 cells with increasing ratios of aurora kinase A to p53 in independent experiments. Increasing expression of aurora kinase A led to declining steady-state levels of p53, coinciding with less cyclin-dependent kinase inhibitor p21 (**Fig. 3a**). Overexpression of aurora kinase A did not have a similar effect on the level of endogenous and ectopically expressed p21 in the absence of p53 (**Supplementary Fig. 3** online), suggesting that destabilization of p53 after overexpression of aurora kinase A affects downstream p53-transactivated effectors, such as p21. The levels of p27, also regulated by ubiquitin-proteasome degradation system[31], and a control GFP did not change in these experiments, indicating that aurora kinase A–mediated destabilization of p53 is not a nonspecific phenomenon. We assayed the effect of aurora kinase

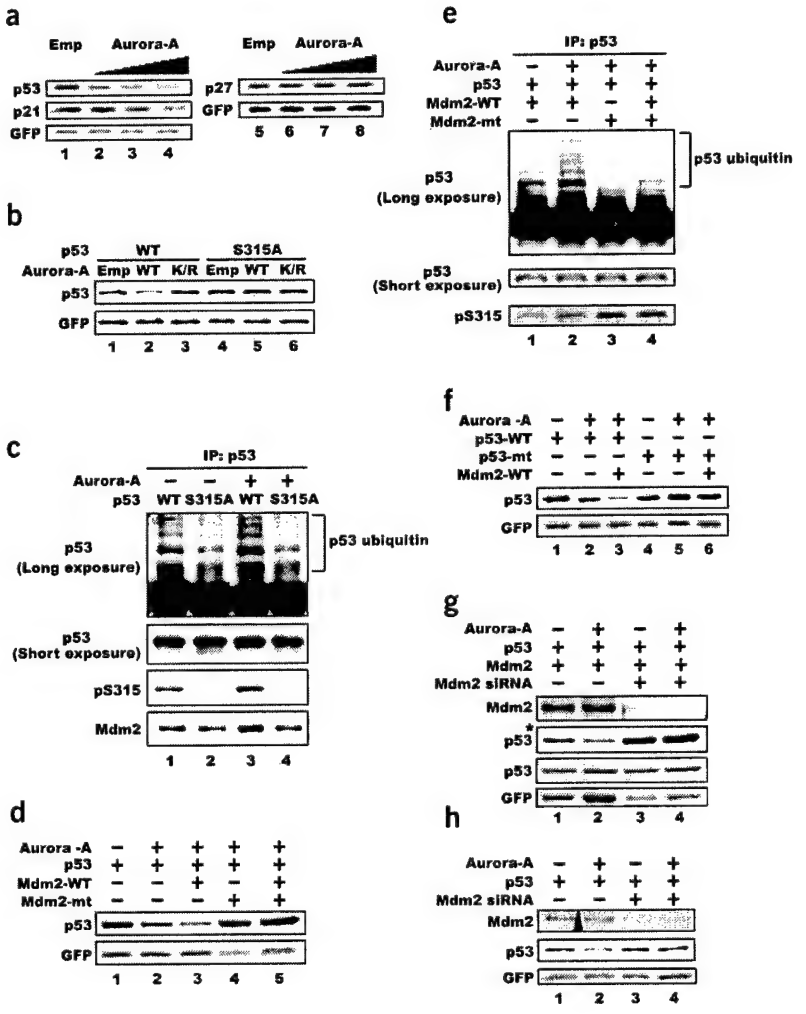

Figure 3 Phosphorylation by aurora kinase A destabilizes p53. (**a**) p53 or p27 was cotransfected with empty vector (Emp) and GFP (lane 1) or with different amounts of aurora kinase A and GFP into H1299 cells (lane 2–4). Twenty-four hours after transfection, aliquots of the same total cell lysates were immunoblotted with the indicated antibodies. Similar GFP expression indicates comparable transfection efficiency (bottom). (**b**) Wild-type p53 (WT; lanes 1–3) or p53 S315A (lane 4–6) was cotransfected with empty vector (Emp; lanes 1 and 4), with wild-type aurora kinase A (WT; lanes 2 and 5) or with aurora kinase A K162R (K/R; lanes 3 and 6) into H1299 cells and analyzed as in **a**. (**c**) Mdm2 was cotransfected with wild-type p53 (WT; lane 1), with p53 S315A (lane 2), with wild-type aurora kinase A and wild-type p53 (lane 3) or with wild-type aurora kinase A and p53 S315A (lane 4) into H1299 cells, and cells were treated with protease inhibitor N-acetyl-Leu-Leu-Norleucinal for 6 h before harvest. Twenty-four hours after transfection, p53 was immunoprecipitated (IP) with antibody to p53 and then immunoblotted with antibody to p53. The same membrane was stripped and reprobed with indicated antibodies. pS315, p53 phosphorylated at Ser315. Short exposure shows the unubiquitinated single band of p53. Long exposure of the same membrane shows multiple ubiquitinated bands of p53 in addition to the single unubiquitinated band seen after short exposure. (**d**) p53 was cotransfected with empty vector (lane 1), with aurora kinase A (lane 2), with aurora kinase A and wild-type Mdm2 (WT; lane 3), with aurora kinase A and a ubiquitination-defective Mdm2 mutant (mt; lane 4) or with aurora kinase A, wild-type Mdm2 and mutant Mdm2 (lane 5) into H1299 cells and analyzed as in **a**. (**e**) p53 was cotransfected with wild-type Mdm2 (WT; lane 1), with aurora kinase A and wild-type Mdm2 (lane 2), with aurora kinase A and mutant Mdm2 (mt; lane 3) or with aurora kinase A, wild-type Mdm2 and mutant Mdm2 (lane 4) into H1299 cells and analyzed as in **c**. IP, immunoprecipitation. Short exposure shows the unubiquitinated single band of p53. Long exposure of the same membrane shows multiple ubiquitinated bands of p53 in addition to the single unubiquitinated band seen after short exposure. (**f**) Wild-type p53 (WT; lanes 1–3) or a p53 mutant that does not bind Mdm2 (mt; lanes 4–6) was cotransfected with empty vector (lanes 1 and 4), with aurora kinase A (lanes 2 and 5) or with aurora kinase A and wild-type Mdm2 (lanes 3 and 6) and analyzed as in **a**. (**g**) H1299 cells transfected with control siRNA duplex (GL2; lanes 1 and 2) or siRNA duplex targeting Mdm2 (lanes 3 and 4). Twenty-four hours after transfection, p53 and Mdm2 were cotransfected with either empty vector (lanes 1 and 3) or with aurora kinase A (lanes 2 and 4) for 24 h and cells were immunoblotted with indicated antibodies. p53* (second row) shows the normalized amount of p53 in the four samples. Normalization was done after densitometric analyses of p53 (third row) and GFP (fourth row) band intensities in each lane, using Scion Image and NIH Image software. (**h**) H1299 cells transfected with control siRNA duplex (GL2; lanes 1 and 2) or Mdm2 siRNA duplex (lanes 3 and 4) for 24 h were subjected to cotransfection with p53 (lanes 1 and 3) or with p53 and aurora kinase A together (lanes 2 and 4). After 24 h, cells were analyzed as in **a**.

A–mediated phosphorylation on the stability of p53 by expressing wild-type or S315A variants of p53 with wild-type or kinase-inactive mutants of aurora kinase A in H1299 cells. Only wild-type p53 was destabilized in the cells expressing wild-type aurora kinase A, suggesting that Ser315 phosphorylation by aurora kinase A facilitates degradation of p53 (**Fig. 3b**).

Because degradation of p53 predominantly involves Mdm2-mediated ubiquitination, we assayed ubiquitination of p53 in H1299 cells cotransfected with Mdm2 and either empty vector or vector expressing aurora kinase A in combination with wild-type or S315A mutant p53. In cells expressing wild-type p53, we observed substantially more ubiquitination in the presence of aurora kinase A than in presence of the empty vector. We observed moderate ubiquitination in cells transfected with the empty vector, probably as a result of phosphorylation of p53 by endogenous aurora kinase A. We observed less ubiquitination of p53 in cells expressing the S315A mutant p53 (**Fig. 3c**). The difference in ubiquitination was not due to differences in amount of p53, as comparable levels of p53 were immunoprecipitated from all four transfections. We also noted greater binding of Mdm2 to highly ubiquitinated p53 in cells expressing aurora kinase A (**Fig. 3c**). Consistent with the levels of ubiquitinated p53, bound Mdm2 was more abundant in the cells transfected with empty vector and expressing wild-type p53 than in those expressing S315A mutant p53, possibly owing to phosphorylation of wild-type p53 by endogenous aurora kinase A.

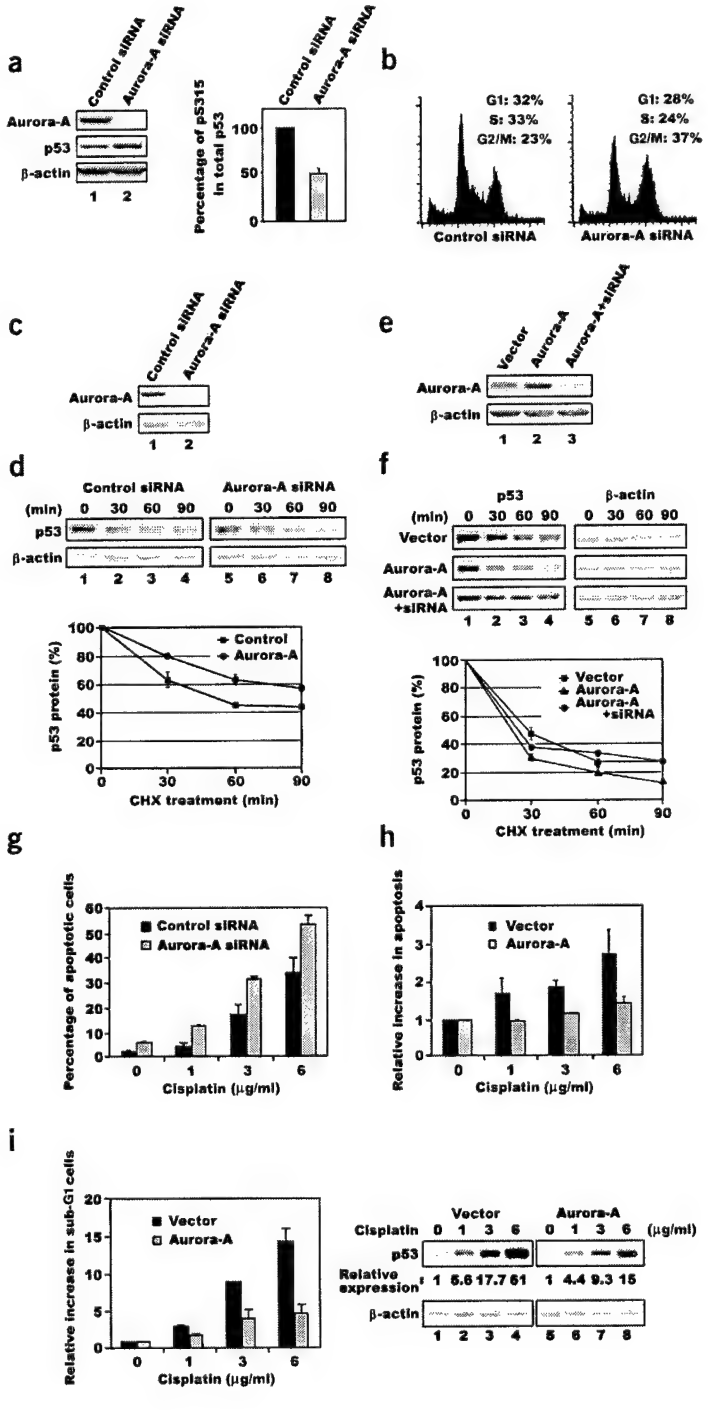

Figure 4 Effect of aurora kinase A expression on p53 stability and function *in vivo*. (**a**) Lysates from U2-OS cells transfected with control siRNA duplex (GL2; lane 1) or siRNA duplex targeting aurora kinase A (lane 2) for 48 h were immunoblotted with indicated antibodies. The same lysates were immunoprecipitated with antibody to p53 and immunoblotted with the indicated antibodies. The relative ratio of p53 phosphorylated at Ser315 (pS315) to total immunoprecipitated p53 was then estimated. (**b**) Cell cycle in **a** was analyzed by FACS. (**c**) Lysates from MCF7 cells transfected with control siRNA duplex (GL2; lane 1) or siRNA duplex targeting aurora kinase A (lane 2) for 72 h were analyzed as in **a**. (**d**) Lysates from MCF7 cells transfected with siRNA for 72 h as in **c** were collected at the indicated time points after addition of cycloheximide (CHX) and subjected to immunoblotting with the indicated antibodies. The amount of p53 was quantified by densitometry and is shown relative to the amount of p53 expressed in absence of cycloheximide. (**e**) Lysates from a stable clone expressing vector (lane 1), a stable clone expressing aurora kinase A (lane 2) and a stable clone expressing aurora kinase A treated with siRNA duplex (lane 3) were analyzed as in **a**. (**f**) Cells in **e** were treated with cycloheximide (CHX) and analyzed as in **d**. (**g**) MCF7 cells transfected with siRNA duplex for 48 h were treated with the indicated concentrations of cisplatin, and 24 h later the number of apoptotic cells was counted. (**h**) MCF7 cells were transfected with vector and GFP together or aurora kinase A and GFP together for 48 h, then treated with cisplatin and analyzed as in **g**. (**i**) Stable clones expressing vector and aurora kinase A were treated with cisplatin for 24 h and the sub-G1 cell population was analyzed by FACS. Expression levels of p53 in the same cells was analyzed as in **a**. The amount of p53 in the control and the cisplatin-treated cells was quantified to assess the relative p53 expression in the cisplatin-treated cells.

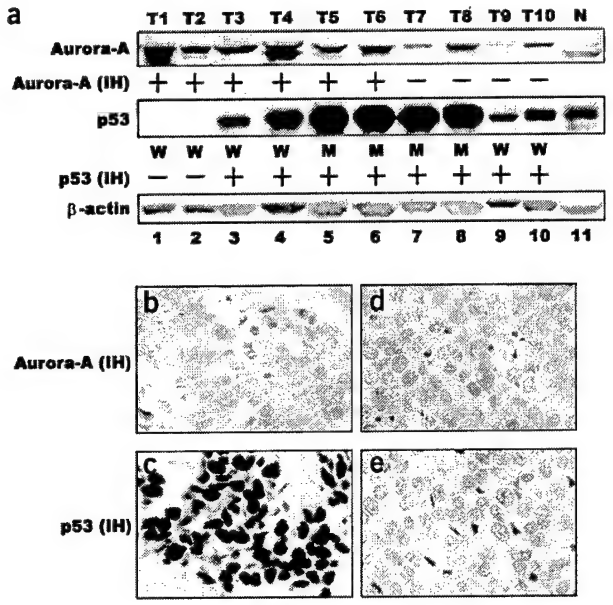

Figure 5 Steady-state level of aurora kinase A and p53 in human bladder tumor samples. (**a**) Expression levels of aurora kinase A (top), p53 (middle) and β-actin (bottom) in bladder tumor tissues (T1–T10; lanes 1–10) and in a normal bladder epithelial cells (N; lane 11). Intensity of immunohistochemical (IH) staining of each tumor specimen compared with normal tissue is represented as follows: –, no detectable expression or similar expression; +, higher expression. W, wild-type p53; M, mutant p53. (**b–e**) Immunohistochemical (IH) staining of tumor specimens with antibody to aurora kinase A (**b**,**d**) and antibody to p53 (**c**,**e**). **b** and **c** represent the same sample, and **d** and **e** represent the same sample.

To further investigate the role of Mdm2 in destabilization of p53 phosphorylated by aurora kinase A, we cotransfected H1299 cells with either mutant Mdm2 (C464A) lacking ubiquitination activity[32] or wild-type Mdm2 and aurora kinase A. The level of p53 was low in cells transfected with wild-type Mdm2 but unaltered in cells transfected with mutant Mdm2 compared with control cells not transfected with Mdm2 (**Fig. 3d**). Mutant Mdm2 also had a dominant negative effect of stabilizing p53 in the presence of aurora kinase A.

We further documented the role of aurora kinase A in Mdm2-mediated ubiquitination of p53 using ubiquitination assays on cells transfected with the same combinations of expression constructs described above (**Fig. 3e**). Ubiquitinated p53 in cells expressing aurora kinase A, p53 and wild-type Mdm2 was much more abundant than in cells expressing mutant Mdm2. As expected, ubiquitination of p53 was minimal in the absence of aurora kinase A and was undetectable in cells expressing mutant Mdm2. Mutant p53 (L22Q and W23S) that cannot interact with Mdm2 (ref. 33) was also not destabilized when expressed with aurora kinase A and Mdm2 (**Fig. 3f**). Silencing of Mdm2 with small interfering RNA (siRNA) in cells with transfected (**Fig. 3g**) and endogenous (**Fig. 3h**) Mdm2 inhibited destabilization of p53 in the presence of aurora kinase A. Absence of a perceptible increase in the amount of p53 after silencing of Mdm2 by siRNA (**Fig. 3h**), which seems to conflict with the existing model of p53 regulation, may reflect the fact that proliferating cells can tolerate only limited amount of p53. These results, taken together, indicate that Mdm2-mediated ubiquitination has a central role in the destabilization of p53 induced by aurora kinase A.

Phosphorylation of p53 at Ser315 affects cell cycle

Because p53 is a crucial regulator of cell cycle progression and DNA damage–induced checkpoint response in mammalian cells[30], we investigated whether inhibition of physiological levels of aurora kinase A with siRNA affects stability of p53 and, consequently, p53-regulated pathways in U2-OS and MCF7 cells with wild-type p53. Treatment of U2-OS cells for 48 h with aurora kinase A siRNA resulted in substantial depletion of aurora kinase A, which was directly correlated with an increase in the steady-state level of p53 and inversely correlated with the amount of p53 phosphorylated at Ser315 (**Fig. 4a**). These cells also had a larger G2-M population of 37%, compared with 23% in cells treated with control siRNA (**Fig. 4b**). This growth arrest or delay in the G2-M phase after depletion of aurora kinase A could be due to stabilization of p53. The lack of a similar growth-inhibitory effect in p53-deficient H1299 and Saos-2 cells depleted of aurora kinase A (data not shown) supports this conclusion.

We then assessed the stability of p53 in MCF7 parental cells and in MCF7 cells stably transfected with aurora kinase A with and without silencing of aurora kinase A by exposure to cycloheximide, a translational inhibitor, in time-course experiments. Treatment with aurora kinase A siRNA for 72 h almost completely inhibited expression of aurora kinase A (**Fig. 4c,e**). We estimated the relative amount of p53 in cells exposed to cycloheximide for 30, 60 and 90 min and found consistently higher levels of p53 in cells treated with aurora kinase A siRNA than in cells treated with a control siRNA. Treatment with cycloheximide for 90 min decreased p53 level by almost 60% in the control cells but only by ~40% in cells with silenced aurora kinase A (**Fig. 4d**), indicating that the degradation rate of p53 was greater in cells expressing aurora kinase A. We observed a similar phenomenon in cells overexpressing aurora kinase A: silencing of aurora kinase A in these cells stabilized p53 to almost the same extent as seen in control cells (**Fig. 4f**). These results suggest that expression of aurora kinase A at physiological levels *in vivo* mediates degradation of p53 and that this effect is enhanced in cells overexpressing aurora kinase A, possibly causing abrogation of p53-mediated checkpoint response pathways.

Aurora kinase A affects p53-mediated apoptosis

We investigated whether aurora kinase A affects p53-induced apoptosis in response to cisplatin-induced DNA damage in MCF7 cells. Silencing of aurora kinase A with siRNA substantially increased the incidence of apoptosis in these cells. Treatment with 6 μg ml^{-1} cisplatin increased the incidence of apoptosis by ~20% in cells with silenced aurora kinase A over that observed in cells transfected with a control siRNA (**Fig. 4g**). The lack of a similar increase in apoptotic response in p53-deficient H1299 cells treated with cisplatin (data not shown) indicated that the apoptotic response in MCF7 cells treated with cisplatin was a reflection of the effect of aurora kinase A on stability of p53. Consistent with its role as an inhibitor of p53 function, overexpression of aurora kinase A in transiently transfected cells inhibited p53-induced apoptotic response after treatment with cisplatin (**Fig. 4h**). Based on the number of sub-G1 DNA-harboring cells generated, cells stably transfected with aurora kinase A were also resistant to cisplatin-induced apoptosis. Substantially less induction of p53 in these cells corroborated the role of aurora kinase A as an inhibitor of p53-induced apoptotic response in DNA-damaged cells (**Fig. 4i**). The apoptotic response was not mediated through the two p53 homologous family members p63 and p73, as cotransfection with increasing amounts of aurora kinase A had no effect on the stability of p63γ and p73α isoforms, implicated in p53 like functions, in untreated (**Supplementary Fig. 3** online) and cisplatin-treated cells (data not shown).

Overexpression of aurora kinase A and low p53 levels

In agreement with the experimental data, we detected a trend between overexpression of aurora kinase A and reduced expression of p53 in human bladder tumors (**Fig. 5**), which frequently overexpress aurora kinase A, according to a recent report[13]. Of 23 tumors analyzed, 18 had no mutations of p53. Of these 18, 15 showed high expression of aurora kinase A, and 10 of these had reduced expression of p53.

DISCUSSION

Our findings indicate that aurora kinase A interacts with and phosphorylates p53 at Ser315, facilitating Mdm2-mediated ubiquitination and destabilization of p53. In view of this finding and the observed growth arrest of cells at G2-M phase after silencing of aurora kinase A, it is logical to suggest that degradation of p53 phosphorylated at Ser315 has physiological relevance related to allowing progression of cells through the normal cell proliferation cycle. Identification of aurora kinase A as an *in vivo* kinase for Ser315 does not rule out possible involvement of other S- and G2-phase cyclin-dependent kinases in the process, as precedents for multiple distinct kinases targeting the same phosphorylation site of p53 (ATM and ATR for Ser15; CK2 and PKR for Ser392) have been reported[34–36].

Phosphorylation of Ser315 has been implicated in enhancing sequence-specific DNA-binding affinity and transactivation function of p53. Total phosphorylation profile, rather than phosphorylation of a single residue, may determine the functional status of p53 at any given stage of the cell cycle. Indeed, the fact that phosphorylation of Ser315 along with Ser33 and Thr81 leads to binding of p53 to prolyl isomerase Pin 1 (refs. 37,38), which stimulates transactivation function and stabilization of p53, indicates that phosphorylation of Ser315 can direct the functional status of p53 to either stabilization or degradation. Selectivity towards a particular response may depend on the total profile of post-translational modifications on p53 and the resultant recruitment of additional proteins required for such a response.

The mechanism by which phosphorylation by aurora kinase A enhances Mdm2-mediated ubiquitination of p53 is not known at this time. Greater binding of Mdm2 to phosphorylated p53 undergoing ubiquitination suggests that p53 phosphorylated by aurora kinase A has greater binding affinity for Mdm2. Ser315 phosphorylation may help oligomerization of p53, which is required for Mdm2-mediated ubiquitination[39]. The ability of Mdm2 to degrade p53 requires shuttling between the nucleus and the cytoplasm[40,41], and inhibition of p53 nuclear export leads to accumulation of ubiquitinated p53 in the nucleus[32]. Localization of aurora kinase A in both nucleus and cytoplasm[42–44] makes it a credible catalyst for p53 ubiquitination.

A recent study using an ectopically expressed transactivation- and oligomerization-defective p53 deletion mutant found that oncogenic activity of aurora kinase A is suppressed by p53 in a transactivation-independent manner[27]. This observation, however, is inconsistent with our model of aurora kinase A function. Because the study cited used a transactivation- and oligomerization-defective p53 deletion mutant for functional assays, the physiological relevance of the reported finding needs to be investigated further.

The most important tumor-suppressor function of p53 involves its ability to induce apoptosis; thus, a negative regulator of p53, such as aurora kinase A, must have a crucial role in tumorigenic transformation of cells. This function of aurora kinase A may explain why overexpression causes oncogenic transformation in mammalian cells and why amplification or overexpression of aurora kinase A is commonly detected in human cancers[8–13]. Notably, our findings also provide a mechanistic explanation for the recently reported role of aurora kinase A as a tumor-susceptibility protein in mouse and human[45]. Overexpression of aurora kinase A resulting in loss of p53 function confers resistance to DNA damage–inducing agents, such as cisplatin, a drug commonly used in cancer chemotherapy. It is, therefore, expected that overexpression of aurora kinase A would be under positive selection in human tumors expressing wild-type p53. The function of aurora kinase A as a p53-destabilizing molecule makes it an important target for developing therapeutic strategies for those human cancers in which aurora kinase A is overexpressed.

METHODS

Mapping of phosphorylation site. We produced GST–aurora kinase A and GST-p53 proteins in BL21 pLys bacteria according to the manufacturer's protocol (Amersham Pharmacia Biotech). We carried out *in vitro* kinase assays as described[14]. We purified ^{32}P-labeled GST-p53 phosphorylated by aurora kinase A *in vitro* by SDS-PAGE and digested it with N-tosyl-L-pheylalanine chloromethyl ketone–trypsin (Sigma). We subjected digested phosphopeptides to phosphorylated amino acid analysis and two-dimensional analysis using the HTLE-7000 electrophoresis system (CBS Scientific) as described[25]. We carried out manual Edman degradation as described[26].

***In vitro* binding assay.** We produced *in vitro*–translated proteins in the presence of ^{35}S-methionine using the TNT coupled transcription/translation kit (Promega). We incubated GST–aurora kinase A or GST-p53 fusion proteins bound to glutathione-Sepharose beads with ^{35}S-labeled p53 or aurora kinase A, respectively, in binding buffer (20 mM Tris (pH 7.4), 100 mM NaCl, 1 mM EDTA, 1 mM dithiothreitol, 0.1% Nonidet P-40) for 1 h at 4 °C and then washed them five times in wash buffer (20 mM Tris (pH 7.4), 100 mM NaCl, 1 mM EDTA, 1 mM dithiothreitol, 0.25% Nonidet P-40, 10% glycerol). We analyzed the bound proteins by SDS-PAGE.

***In vivo* binding assay.** We transfected cells using LipofectAMINE according to the manufacturer's protocol (Invitrogen). We extracted cells with lysis buffer (50 mM Tris (pH 8.0), 20 mM sodium glycerophosphate, 140 mM NaCl, 25 mM NaF, 1 mM phenylmethylsulfonyl fluoride, 1% Nonidet P-40, 0.5 μM okadaic acid, 10 μM Microcystin LR, Protease inhibitor cocktail) 24 h after transfection. We incubated the lysate for 20 min on ice and then centrifuged it at 15,000*g* for 20 min. We used the supernatant for immunoblotting and immunoprecipitation. For immunoprecipitation, we incubated 0.3–2 mg of lysate for 3 h at 4 °C with 15 μl of polyclonal antibody to aurora kinase A conjugated to protein G-agarose or 5 μg of monoclonal antibody to p53 (Ab-6, Oncogene) conjugated to protein G-agarose, washed the immunocomplex four times with lysis buffer and then subjected it to SDS-PAGE.

p53 degradation and ubiquitination assay. We transfected p53-deficient H1299 cells with increasing amounts of either pcDNA3-Flag–tagged aurora kinase A or K162R mutant aurora kinase A together with 0.4 μg of pcDNA3-Flag–tagged p53, S315A mutant p53 or L22Q/W23S double mutant p53; pCMV-Mdm2 or C464A mutant Mdm2; pCEP4-p27, pcDNA3-empty vector and pEGFP-empty vector in separate transfections. We detected levels of p53, p21, p27 and GFP by immunoblotting with the respective antibodies. For this purpose, we used antibody to p21 F-5 (Santa Cruz), antibody to p27 F-8 (Santa Cruz) and antibody to GFP Living Colors A.v. Peptide (Clontech). To evaluate ubiquitination of p53, we treated transfected H1299 cells for 6 h with a proteasome inhibitor LLnL (50 μM; Sigma), collected them and extracted them with lysis buffer. We immunoprecipitated the lysate with monoclonal antibody to p53 (Ab-6) and then resolved it by SDS–PAGE (8% gel) and analyzed it by immunoblotting with antibody to p53 (Ab-6), antibody to p53 phosphorylated at Ser315 and monoclonal antibody to Mdm2 (Ab-1, Oncogene Science). To assess stability of p53, we treated MCF7 cells with 80 μg ml^{-1} of cycloheximide for indicated times.

siRNA, stable clone and cisplatin treatment. We carried out siRNA experiments for aurora kinase A and Mdm2 as previously described[46,47]. We obtained aurora kinase A stable transfectants by transfecting pcDNA3–wild-type aurora kinase A to MCF7 cells and then selecting the cells in the presence of G418 for 3 weeks. We added cisplatin to the culture medium for 24 h at indicated concentrations. For apoptosis analysis of siRNA-transfected cells, we fixed the cells in 3.7% formaldehyde, stained them with DAPI and counted the nuclear morphology of at least

500 cells under the fluorescence microscope. For FACS analysis of siRNA-transfected cells and stable transfectants, we stained the cells with propidium iodide and analyzed them by Becton Dickinson FACSCAN flow cytometer[48].

Bladder tissue samples. We analyzed the expression levels of aurora kinase A kinase and p53 in 23 bladder tumor tissues and 2 normal tissues by immunoblotting and immunohistochemistry as described[13]. We obtained frozen tissue samples from the interdepartmental tissue repository at the University of Texas M.D. Anderson Cancer Center. The tissue samples were collected under the approved institutional laboratory protocols and all individuals from whom samples were collected signed the informed. consent. We isolated exon 5–9 of *TRP53* (encoding p53) from all tumor samples, amplified the region and directly sequenced it by applying the cycle sequencing dye terminator protocol (PE Applied Biosystems).

Note: Supplementary information is available on the Nature Genetics website.

ACKNOWLEDGMENTS

We thank B. Vogelstein and C. Lengauer for Mdm2, p21 and p27 expression constructs; T. Hupp and E. Appella for antibodies specific to p53 phosphorylated at Ser315; J. Dai for BT549 cells; H. Grossman for normal human uroepithelial cells; J. Liu for help with the two-dimensional protein gel and analysis of phosphorylated amino acids; and G. Lozano, J. Barboza and J. Carter for helpful discussion and critical reading of the manuscript. This work was supported by grants from the US National Institutes of Health, US Department of Defense Breast Cancer Research Program, and The University of Texas M.D. Anderson Cancer Center Human Cancer Genetics Development Funds (to S.S.). DNA sequencing was done at the M.D. Anderson Cancer Center DNA sequencing facility, supported by a US National Institutes of Health Core grant.

COMPETING INTERESTS STATEMENT

The authors declare that they have no competing financial interests.

Received 5 October; accepted 12 November 2003
Published online at http://www.nature.com/naturegenetics/

1. Nigg, E.A. Mitotic kinases as regulators of cell division and its checkpoints. *Nat. Rev. Mol. Cell. Biol.* **2**, 21–32 (2001).
2. Glover, D.M., Leibowitz, M.H., McLean, D.A. & Parry, H. Mutations in *aurora* prevent centrosome separation leading to the formation of monopolar spindles. *Cell* **81**, 95–105 (1995).
3. Chan, C.S. & Botstein, D. Isolation and characterization of chromosome-gain and increase-in-ploidy mutants in yeast. *Genetics* **135**, 677–691 (1993).
4. Bischoff, J.R. & Plowman, G.D. The Aurora/Ipl1p kinase family: regulators of chromosome segregation and cytokinesis. *Trends Cell Biol.* **9**, 454–459 (1999).
5. Giet, R. & Prigent, C. Aurora/Ipl1p-related kinases, a new oncogenic family of mitotic serine-threonine kinases. *J. Cell Sci.* **112**, 3591–3601 (1999).
6. Goepfert, T.M. & Brinkley, B.R. The centrosome-associated Aurora/Ipl-like kinase family. *Curr. Top. Dev. Biol.* **49**, 331–342 (2000).
7. Hirota, T. *et al.* Aurora-A and an interacting activator, the LIM protein Ajuba, are required for mitotic commitment in human cells. *Cell* **114**, 585–598 (2003).
8. Zhou, H. *et al.* Tumour amplified kinase STK15/BTAK induces centrosome amplification, aneuploidy and transformation. *Nat. Genet.* **20**, 189–193 (1998).
9. Bischoff, J.R. *et al.* A homologue of *Drosophila* aurora kinase is oncogenic and amplified in human colorectal cancers. *EMBO J.* **17**, 3052–3065 (1998).
10. Sen, S., Zhou, H. & White, R.A. A putative serine/threonine kinase encoding gene BTAK on chromosome 20q13 is amplified and overexpressed in human breast cancer cell lines. *Oncogene* **14**, 2195–2200 (1997).
11. Tanaka, T. *et al.* Centrosomal kinase AIK1 is overexpressed in invasive ductal carcinoma of the breast. *Cancer Res.* **59**, 2041–2044 (1999).
12. Miyoshi, Y., Iwao, K., Egawa, C. & Noguichi, S. Association of centrosomal kinase STK15/BTAK mRNA expression with chromosomal instability in human breast cancers. *Int. J. Cancer* **92**, 370–373 (2001).
13. Sen, S. *et al.* Amplification/overexpression of a mitotic kinase gene in human bladder cancer. *J. Natl. Cancer Inst.* **94**, 1320–1329 (2002).
14. Katayama, H., Zhou, H., Li, Q., Tatsuka, M. & Sen, S. Interaction and feedback regulation between STK15/BTAK/aurora-A kinase and protein phosphatase 1 through mitotic cell division cycle. *J. Biol. Chem.* **276**, 46219–46224 (2001).
15. Fukasawa, K., Choi, T., Kuriyama, R., Rulong, S. & VandeWonde, G.F. Abnormal centrosome amplification in the absence of p53. *Science* **271**, 1744–1747 (1996).
16. Bischoff, F.Z. *et al.* Spontaneous abnormalities in normal fibroblasts from patients with Li-Fraumeni cancer syndrome: aneuploidy and immortalization. *Cancer Res.* **50**, 7979–7984 (1990).
17. Kubbutat, M.H., Jones, S.N. & Vousden K.H. Regulation of p53 stability by Mdm2. *Nature* **387**, 299–303 (1997).
18. Shieh, S.Y., Ikeda, M., Taya, Y. & Prives, C. DNA damage-induced phosphorylation of p53 alleviates inhibition by Mdm2. *Cell* **91**, 325–334 (1997).
19. Shieh, S.Y., Taya, Y. & Prives, C. DNA damage-inducible phosphorylation of p53 at N-terminal sites including a novel site, Ser20, requires tetramerization. *EMBO J.* **18**, 1815–1823 (1999).
20. Shieh, S.Y., Ahn, J., Tamai, K., Taya, Y. & Prives, C. The human homologs of checkpoint kinases Chk1 and Cds1 (Chk2) phosphorylate p53 at multiple DNA damage-inducible sites. *Genes Dev.* **14**, 289–300 (2000).
21. Sakaguchi, K. *et al.* DNA damage activates p53 through a phosphorylation-acetylation cascade. *Genes Dev.* **12**, 2831–2841 (1998).
22. Shaw, P., Freeman, J., Bovey, R. & Iggo, R. Regulation of specific DNA binding by p53: evidence for a role for O-glycosylation and charged residues at the carboxy-terminus. *Oncogene* **12**, 921–930 (1996).
23. Rodriguez, M. S., Dargemont, C. & Hay, R.T. SUMO-1 conjugation in vivo requires both a consensus modification motif and nuclear targeting. *J. Biol. Chem.* **276**, 12654–12659 (2001).
24. Bech-Otschir, D. *et al.* COP9 signalosome-specific phosphorylation targets p53 to degradation by the ubiquitin system. *EMBO J.* **20**, 1630–1639 (2001).
25. Liu, J. *et al.* Inhibition of Bcr serine kinase by tyrosine phosphorylation. *Mol. Cell. Biol.***16**, 998–1005 (1996).
26. Zhou, B.P. *et al.* Cytoplasmic localization of p21Cip1/WAF1 by Akt-induced phosphorylation in HER-2/neu-overexpressing cells. *Nat. Cell Biol.* **3**, 245–252 (2001).
27. Chen, S.S., Chang, P.C., Cheng, Y.W., Tang, F.M.& Lin, Y.S. Suppression of the STK15 oncogenic activity requires a transactivation-independent p53 function. *EMBO J.* **21** 4491–4499 (2002).
28. Wang, Y. & Prives, C. Increased and altered DNA binding of human p53 by S and G2/M but not G1 cyclin-dependent kinases. *Nature* **376**, 88–91 (1995).
29. Sakaguchi, K. *et al.* Phosphorylation of serine 392 stabilizes the tetramer formation of tumor suppressor protein p53. *Biochemistry* **36**, 10117–10124 (1997).
30. Vogelstein, B., Lane, D. & Levine, A.J. Surfing the p53 network. *Nature* **408**, 307–310 (2000).
31. Boehm, M. *et al.* A growth factor-dependent nuclear kinase phosphorylates p27(Kip1) and regulates cell cycle progression. *EMBO J.* **21**, 3390–3401 (2002).
32. Geyer, R.K., Yu, Z.K. & Maki, C.G. The Mdm2 RING-finger domain is required to promote p53 nuclear export. *Nat. Cell Biol.* **2**, 569–573 (2000).
33. Lin, J., Chen, J., Elenbaas, B. & Levine, A.J. Several hydrophobic amino acids in the p53 amino-terminal domain are required for transcriptional activation, binding to mdm-2 and the adenovirus 5 E1B 55-kD protein. *Genes Dev.* **8**, 1235–1246 (1994).
34. Banin, S. *et al.* Enhanced phosphorylation of p53 by ATM in response to DNA damage. *Science* **281**, 1674–1677 (1998).
35. Tibbetts, R.S. *et al.* A role for ATR in the DNA damage-induced phosphorylation of p53. *Genes Dev.* **13**, 152–157 (1999).
36. Cuddihy, A.R., Wong, A.H., Tam, N.W., Li, S. & Koromilas, A.E. The double-stranded RNA activated protein kinase PKR physically associates with the tumor suppressor p53 protein and phosphorylates human p53 on serine 392 in vitro. *Oncogene* **18**, 2690–2702 (1999).
37. Zheng, H. *et al.* The prolyl isomerase Pin1 is a regulator of p53 in genotoxic response. *Nature* **419**, 849–853 (2002).
38. Zacchi, P. *et al.* The prolyl isomerase Pin1 reveals a mechanism to control p53 functions after genotoxic insults. *Nature* **419**, 853–857 (2002).
39. Maki, C.G. Oligomerization is required for p53 to be efficiently ubiquitinated by Mdm2. *J. Biol. Chem.* **274**, 16531–16535 (1999).
40. Woods, D.B. & Vousden, K.H. Regulation of p53 function. *Exp. Cell. Res.* **264**, 56–66 (2001).
41. Momand, J., Wu, H.H. & Dasgupta, G. Mdm2—master regulator of the p53 tumor suppressor protein. *Gene* **242**, 15–29 (2000).
42. Kiat, L.S., Hui, K.M. & Gopalan, G. aurora-A kinase interacting protein (AIP), a novel negative regulator of human aurora-A kinase. *J. Biol. Chem.* **277**, 45558–45565 (2002).
43. Crosio, C. *et al.* Mitotic phosphorylation of histone H3: spatio-temporal regulation by mammalian Aurora kinases. *Mol. Cell. Biol.* **22**, 874–885 (2002).
44. Stenoien, D.L., Sen, S., Mancini, M.A. & Brinkley, B.R. Dynamic association of a tumor amplified kinase, Aurora-A, with the centrosome and mitotic spindle. *Cell Motil. Cytoskeleton* **55**, 134–146 (2003).
45. Ewart-Toland, A. *et al.* Identification of *Stk6/STK15* as a candidate low-penetrance tumor-susceptibility gene in mouse and human. *Nat. Genet.* **34**, 403–412 (2003).
46. Kufer, T.A. *et al.* Human TPX2 is required for targeting Aurora-A kinase to the spindle. *J. Cell Biol.* **158**, 617–623 (2002).
47. Brès, V. *et al.* A non-proteolytic role for ubiquitin in Tat-mediated transactivation of the HIV-1 promoter. *Nature Cell Biol.* **8**, 754–761 (2003).
48. Sen, S. *et al.* Expression of a gene encoding a tRNA synthetase like protein is enhanced in tumorigenic human myeloid leukemia cells and is cell cycle stage and differentiation dependent. *Proc. Natl. Acad. Sci. USA* **94**, 6164–6169 (1997).

Cell Motility and the Cytoskeleton 55:134–146 (2003)

Dynamic Association of a Tumor Amplified Kinase, Aurora-A, With the Centrosome and Mitotic Spindle

D. L. Stenoien,[1]* S. Sen,[2] M.A. Mancini,[1] and B. R. Brinkley[1]

[1]*Department of Molecular and Cellular Biology, Baylor College of Medicine, Houston, Texas*
[2]*Department of Molecular Pathology, University of Texas M.D. Anderson Cancer Center, Houston, Texas*

Aurora-A kinase, also known as STK15/BTAK kinase, is a member of a serine/threonine kinase superfamily that includes the prototypic yeast Ipl1 and Drosophila aurora kinases as well as other mammalian and non-mammalian aurora kinases involved in the regulation of centrosomes and chromosome segregation. The Aurora-A gene is amplified and overexpressed in a wide variety of human tumors. Aurora-A is centrosome-associated during interphase, and binds the poles and half-spindle during mitosis; its over-expression has been associated with centrosome amplification and multipolar spindles. GFP-Aurora-A was used to mark centrosomes and spindles, and monitor their movements in living cells. Centrosome pairs labeled with GFP-Aurora-A are motile throughout interphase undergoing oscillations and tumbling motions requiring intact microtubules and ATP. Fluorescence recovery after photobleaching (FRAP) was used to examine the relative molecular mobility of GFP-Aurora-A, and GFP-labeled α-tubulin, γ-tubulin, and NuMA. GFP-Aurora-A rapidly exchanges in and out of the centrosome and mitotic spindle ($t_{1/2}$~3 sec); in contrast, both tubulins are relatively immobile indicative of a structural role. GFP-NuMA mobility was intermediate in both interphase nuclei and at the mitotic spindle ($t_{1/2}$~23–30 sec). Deletion mapping identifies a central domain of Aurora-A as essential for its centrosomal localization that is augmented by both the amino and the carboxyl terminal ends of the protein. Interestingly, amino or carboxy terminal deletion mutants that maintained centrosomal targeting exhibited significantly slower molecular exchange. Collectively, these studies contrast the relative cellular dynamics of Aurora-A with other cytoskeletal proteins that share its micro-domains, and identify essential regions required for targeting and dynamics. Cell Motil. Cytoskeleton 55: 134–146, 2003.

Key words: centrosome; mitotic spindle; GFP-Aurora A kinase; FRAP

INTRODUCTION

The aurora serine/threonine kinases regulate a variety of events in mitosis and cell proliferation in eukaryotic cells [reviewed in Goepfert and Brinkley, 2000; Katayama et al., 2003]. First identified in budding yeast as Ipl1 [Chan and Botstein, 1993], several aurora kinase homologs have been identified in Drosophila, Xenopus, *C. elegans*, mouse, and various other mammals, including humans [Katayama et al., 2003]. In humans, the STK15 gene product, Aurora-A kinase, is specifically associated with the centrosome of interphase cells [Zhou et al., 1998] as well as with the spindle during mitosis. Aurora-A is a putative oncogene that is overexpressed in many human tumors and can induce centrosome ampli-

Contract grant sponsor: NIH; Contract grant numbers: CA 41424, CA 64255, CA 61979, CA 89716; Contract grant sponsor: US Department of Defense; Contract grant number: DAMD 17-01-1-0302.

*Correspondence to: David L. Stenoien, Ph.D., Department of Molecular and Cellular Biology, Baylor College of Medicine, Houston, TX 77030. E-mail: stenoien@bcm.tmc.edu

Received 30 December 2002; Accepted 27 February 2003

Published online 28 April 2003 in Wiley InterScience (www.interscience.wiley.com). DOI: 10.1002/cm.10120

fication and chromosomal instability when transfected into normal, near diploid cells in addition to causing tumorigenic transformation in rodent cells in vitro and in vivo [Zhou et al., 1998; Bischoff et al., 1998]. These findings suggest that Aurora-A may somehow influence centrosome duplication, distribution, and related activities in the cell cycle and account for the phenomenon of centrosome amplification seen in many tumor cells. The regulatory pathway for Aurora-A is not well understood but recent studies suggest that its oncogenic activity involves an interaction with p53 and that Aurora-A mediated centrosome amplification can be suppressed by p53 co-expression experiments [Chen et al., 2002]. Recent studies of a rat mammary tumor model suggest Aurora-A expression may be influenced by hormones with overexpression occurring early in carcinogenesis [Goepfert et al., 2002].

In view of current and recent studies implicating the involvement of Aurora-A in centrosome behavior and related activities of the cell cycle, especially mitosis and oncogenesis, we utilized a live cell approach to analyze the cellular targeting and molecular dynamics of green fluorescent protein-tagged Aurora-A (GFP-Aurora-A). Specifically, we were interested in analyzing the patterns of association of Aurora-A with centrosomes throughout the cell cycle and the dynamics of its association with the mitotic apparatus. In addition to the molecular dynamics of Aurora-A interactions, our experimental design enabled us to analyze and characterize patterns of centrosome movement in normally dividing cells and in cells with centrosome amplification (more than the usual 1-2 centrosomes/cell). We also compared the dynamics of Aurora-A association with that of various other proteins including alpha and gamma tubulin and the nuclear matrix-mitotic apparatus (NuMA) protein known to share micro-domains with Aurora-A in the centrosome and spindle poles [Mountain and Compton, 2000; He et al., 1995; Zheng et al., 1991]. Although fixed cell approaches show specific targeting of Aurora-A to the centrosome/spindle, our live cell approaches show surprisingly high molecular mobility of Aurora-A compared to tubulins and NuMA. The high mobility of Aurora-A suggests a dynamic role in its regulation as anticipated via its kinase activity.

MATERIALS AND METHODS

Vector Construction

A stable cell line expressing GFP-γ-tubulin [Khodjakov and Rieder, 1999] was a kind gift from Conly L. Rieder. GFP-NuMA was a gift from Jeffrey Nickerson. GFP-α-tubulin was purchased from Clontech. To create the GFP-tagged Aurora-A, full-length Aurora-A cDNA was amplified by PCR using pcBTAK3 [Zhou et al., 1998] as a template and the following primers; 5′GATC AGA TCT ATG GAC CGA TCT AAA GAA AAC TGC3′ and 5′GATC GGT ACC CTA AGA CTG TTT GCT AGC TGA TTC3′. The resulting PCR fragment contained a 5′ BglII site prior to the start codon and a KpnI site following the stop codon. This PCR fragment was subcloned into the MCS of pEGFP-C1 (Clontech) using the BglII and KpnI restriction sites to make pEGFP-Aurora-A. HindIII and EcoR1 sites located within the reading frame of Aurora-A were used to replace the majority of the sequence generated by PCR with the wild type Aurora-A sequence from pcBTAK3. The remaining ends of Aurora-A cDNA were sequenced to ensure no PCR errors were generated. To make tetracycline regulated GFP-Aurora-A, pEGFP-Aurora-A was digested with BglII and KpnI and the resulting insert was ligated into pTRE-EGFP-C1 digested with the same two restriction enzymes to generate pTRE-EGFP-Aurora-A. The pTRE-EGFP-C1 vector was generated by amplifying the EGFP sequence from pEGFP-C1 by PCR to place a SacII site prior to the start codon of EGFP. This fragment was inserted into pTRE (Clontech) using the SacII and EcoRI sites. To make GFP tagged Aurora-A deletion mutants, cDNA fragments within the specified domains were amplified with BglII linker primer as the forward primer and EcoRV linker primer as the reverse primer, respectively. Amplified fragments were subcloned into pCR2.1 Topo vector (Invitrogen) for sequencing. After verification of the sequence, the mutant fragments were subcloned into pEGFP vector (Clontech) at BglII site and EcoRV sites.

Cell Culture

HeLa Cells were maintained in OptiMEM media supplemented with 4% FBS and Pen/Strep. HeLa Tet-On cells (Clontech) were maintained in the same media with the exception that normal FBS was replaced with Tet-FBS (Clontech) supplemented with 100 μg/ml G418. Stable cell lines expressing inducible GFP-Aurora-A were grown in the same media supplemented with 100 μg/ml hygromycin.

Live-Cell Analysis and FRAP

Stable cell lines expressing GFP-Aurora-A under the control of the tetracycline response element were created in HeLa Tet-On cells (Clontech) according to the instructions of the supplier, selected microscopically and immunoblotted, and then expanded. Prior to analysis, cells were plated onto 40-mm glass coverslips and treated for 24 h with 4 μg/ml doxycycline. Transient transfection of other plasmids was performed using Fugene (Roche). Prior to analysis, coverslips containing

stably or transiently transfected cells were transferred to a live-cell chamber (Bioptechs, Inc., Butler, PA) with fresh media (20 ml) recirculated via a peristaltic pump and immediately returned to the incubator for at least 30 min to allow the system to equilibrate. Fixed and live cell imaging was performed on a Deltavision restoration microscopy system (Applied Precision, Inc; Photometrics CH350 or Micromax CCDs). For time-lapse recordings through the cell cycle, 10, 0.2 μ Z steps were collected rapidly (using a bin of 2 or 3, generally about 0.1–0.5 sec/image) with 5-min time intervals. Using the DeltaVision software, Z stacks were deconvolved and projected, then used to make a QuickTime movie. Representative data from normal or experimental conditions are shown; each data set type was repeated at least six times. FRAP was performed using a LSM 510 confocal microscope (Carl Zeiss, Inc.) fitted with a 63× objective lens. The live cell chamber and objective lens were continuously monitored and maintained at 37°C. A single Z-section was imaged before and at set time intervals following the bleach. The bleach was performed by setting the laser wavelength to 488 nm for GFP at maximum power for 75 iterations (taking ~1 sec to complete, depending on the size of the bleach area). The fluorescence intensities were determined using LSM software (Carl Zeiss Inc., Laser Scanning Microscope, LSM510, Version 2.5) and data was exported to Excel (Microsoft, Inc., Version 4.0) for analysis. Images were exported as TIF files and final figures were generated using Adobe Photoshop (Adobe Systems Inc, Version 5) and Microsoft Excel. Data Analysis. Using the LSM510 software, a region of interest (ROI) corresponding to the bleach area was marked for analysis in each cell. The bleach and the ROI areas were held constant throughout each experiment. After completion of the photobleach, the signal intensity within the ROI was collected at set time intervals. Intensity values were normalized using the following equation; $It = (Xt - Y)/(Z - Y)$, where I is the normalized intensity at time t, X is the actual intensity at time t, Y is the intensity immediately following the photobleach (when t is equal to zero), and Z is the intensity at the final time point. This sets the initial post-bleach intensity (at $t = 0$ s) to zero and the final intensity (after 40 scans) to 1 arbitrary units. Regression analysis was performed by calculating the least squares fit using the standard first order logarithmic equation; $y = c\ln x + b$, where c is the slope, b is the y-intercept, and ln x is the natural logarithm function of the time and y is the fully normalized intensity at a given time. Due to the normalization of the intensities, the $t_{1/2}$ value can be readily observed from the graph as the time at which the normalized intensity reaches 0.5 arbitrary units.

RESULTS

To establish the living cell dynamics of Aurora-A associated with the centrosome and mitotic spindle, a stable HeLa cell line was generated expressing green fluorescent protein-Aurora-A (GFP-Aurora-A) under the control of the tetracycline response element (TRE). Upon induction with doxycycline (4 μg/ml), GFP-Aurora-A becomes detectable by Western blot within 2 h and reaches maximum expression at ~24 h (Fig. 1A). The expressed GFP-Aurora-A retains the ability to specifically target centrosomes and spindles (Fig. 1B and C) indicating that GFP does not affect Aurora-A localization. In vitro kinase assays show that GFP-Aurora-A also retains enzymatic activity (data not shown). Cells expressing GFP-Aurora-A were followed throughout complete cell cycles (Fig. 2). GFP-Aurora-A localizes to the interphase centrosome and remains there during duplication. After duplication, a single enlarged fluorescent spot defines the centrosome, and major microtubule organizing center (MTOC) in the cytoplasm. Subsequently, the single fluorescent spot separates into two smaller spots, as daughter centrosomes separate and move apart. GFP-Aurora-A associates with the duplicated centrosomes throughout G2 and remains there as they move to opposite spindle poles at the onset of mitosis. Although interpolar microtubules are known to form between separating centrosomes [reviewed in Brinkley and Stubblefield, 1967], GFP-Aurora-A remained intimately associated with the centrosome until the onset of prometaphase, when GFP-Aurora-A was found to abruptly spread from the centrosomes to a zone between the kinetochore and spindle pole (half-spindle) where it remained throughout mitosis until late anaphase when chromosomes moved apart to opposite poles. The spindle localization excluded the interzone between separating anaphase chromosomes. At telophase, GFP-Aurora-A again targeted the centrosome, although at a somewhat diminished level of fluorescence, in each of the newly formed daughter cells. Thus, using, GFP-Aurora-A, we are able to visualize the complete centrosome cycle that includes duplication, movement to opposing poles, spindle generation and separation into the single centrosome found in each daughter cell.

As described by Piel et al. [2000], centrosomes and their component centrioles are mobile during interphase when live cells are analyzed by time-lapse digital microscopy using GFP-tagged centrin. We found similar mobile behavior when centrosomes were marked with GFP-Aurora-A. As shown in Figure 3, when images of a pair of centrosomes in a G2 cell were captured at 5-min intervals, over a period of 145 min, considerable oscillatory motion was noted between daughter centrosomes. Thus, at times, a doublet or single overlapping image was

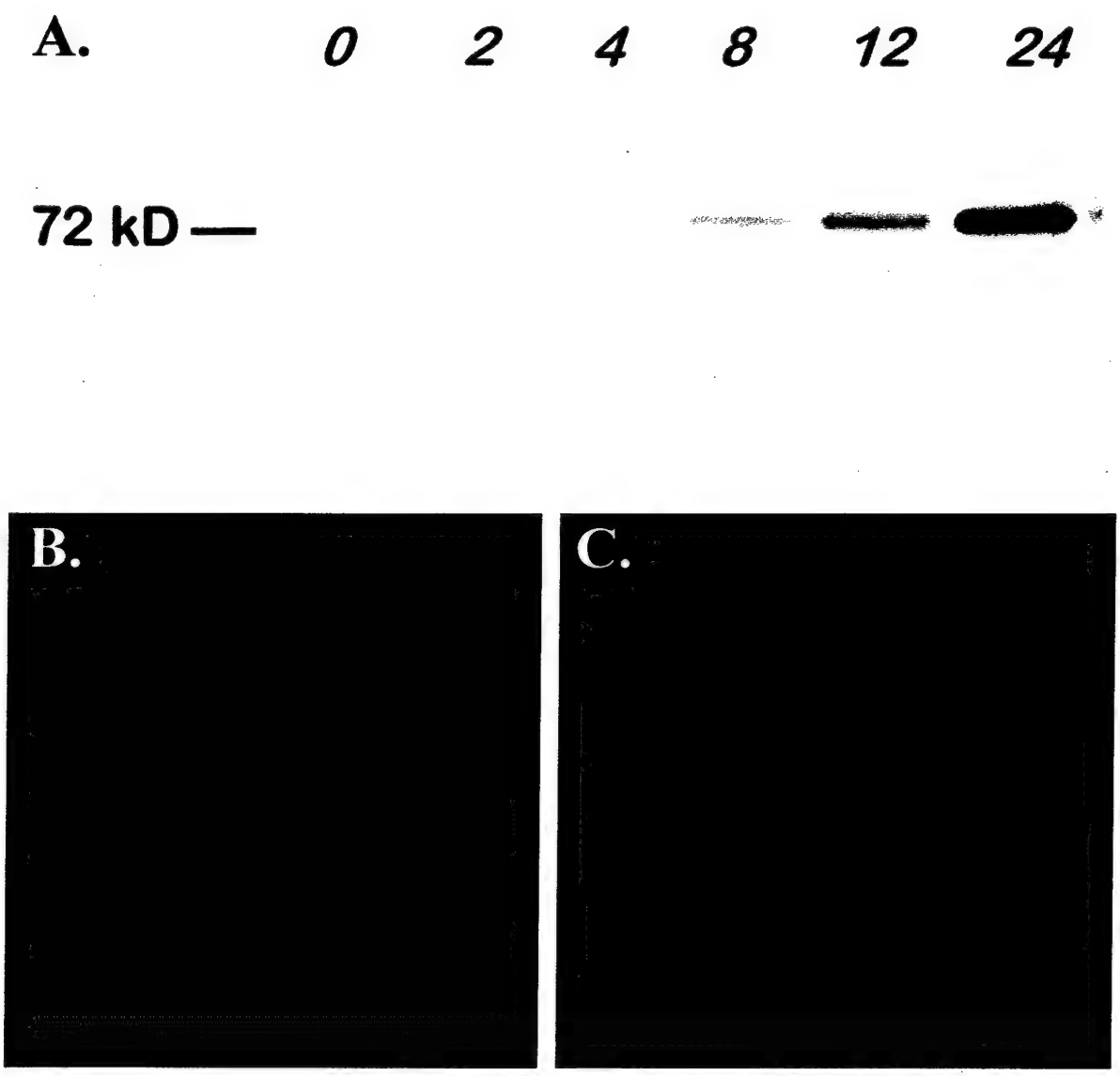

Fig. 1. Regulated expression of GFP-Aurora-A. **A:** GFP-Aurora-A was subcloned into the pTRE vector (Clontech) and a stable cell line was generated in HeLa Tet-on cells. GFP-Aurora-A expression is induced by doxycycline addition and detectable levels of Aurora-A are evident at 2–4 h. Following induction, GFP-Aurora-A (*green*) localizes to centrosomes during interphase and prometaphase (**B**) before moving onto spindles (**C**) during metaphase. DNA is stained with DAPI (*blue*).

detected, but later the daughter centrosomes separated by a distance of several microns and then came back together again where they appeared to collide, forming a doublet or figure eight image only to separate and move apart again. The oscillatory movements were plotted in Figure 3B to show the distance between paired centrosomes over time.

In addition to the oscillatory movements, individual members of a pair of duplicated centrosomes appeared to display a tumbling motion during the oscillations. In addition to the tumbling, the oscillation pattern of movement involving individual centrosomes, the entire centrosome complement (both daughters) could be seen to rotate in a plane approximately 30–40 degrees from an original plane. This pattern of movement continued throughout the G2 phase of the cell cycle until prophase, when centrosomes separated to form opposite spindle poles. Such tumbling and oscillatory motion were not noted during mitosis when spindle poles underwent their typical patterns of movement (i.e., spindle elongation) during the metaphase to anaphase transition.

We analyzed the role of microtubules in centrosome movements by perfusing nocodazole into living

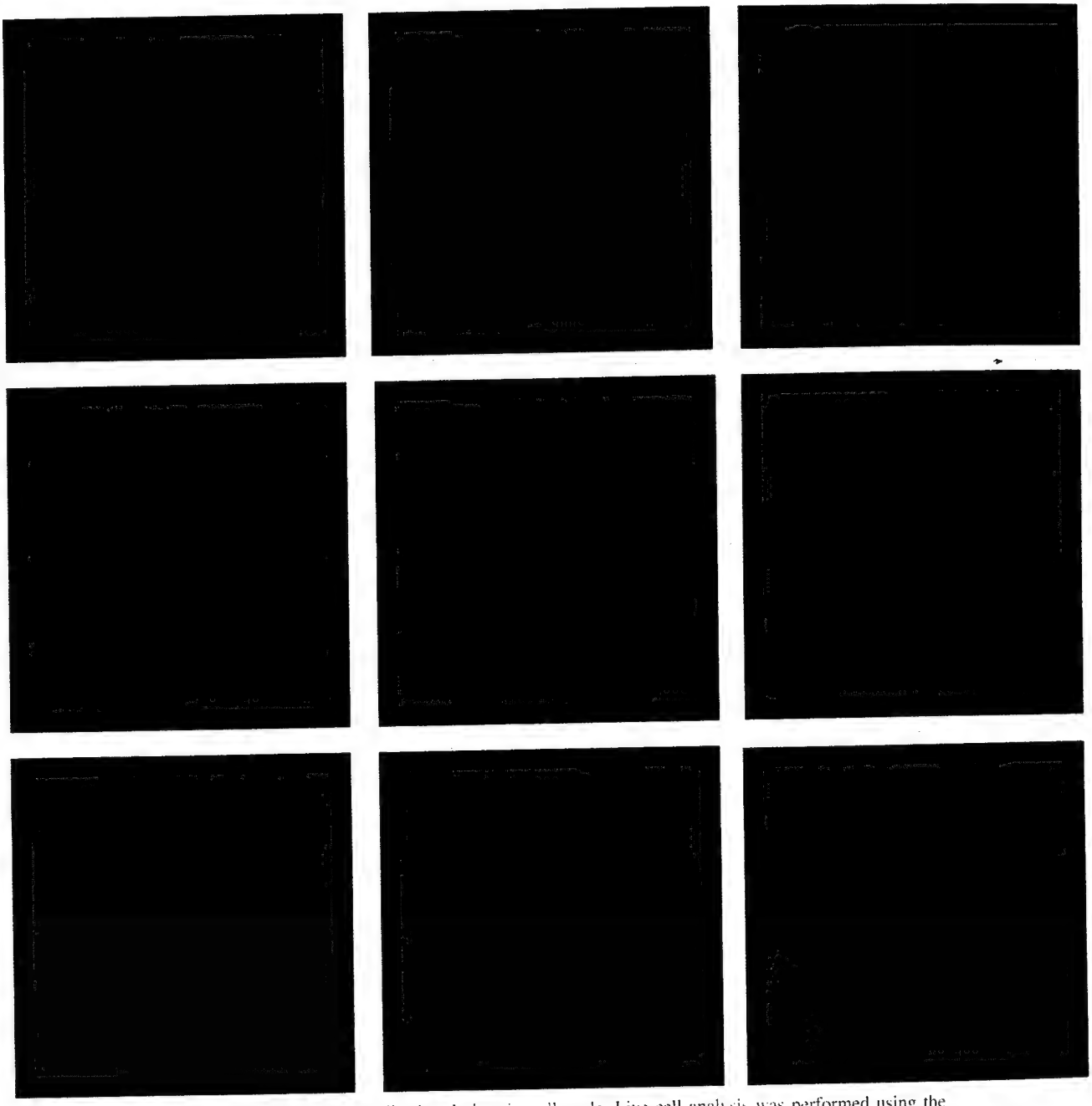

Fig. 2. GFP-Aurora-A Localization during the cell cycle. Live cell analysis was performed using the GFP-Aurora-A stable cell line showing the interactions of Aurora-A with the centrosomes and spindle at different stages of the cell cycle. Aurora-A localizes to a single centrosome that divides, separates to the poles, and eventually forms part of the spindle. Images are shown over a 2-h time frame.

cells as described in Materials and Methods. As noted in Figure 3C, centrosome motion ceased during the period after the inhibitor was perfused into the cells but resumed when removed after chasing with culture media. Under these conditions, the effects of nocodazole appeared to be surprisingly reversible as centrosome movements resumed immediately after the cells were washed. Perfusing the cultures with warm medium alone had no effect on movement (data not shown).

In order to determine if centrosome oscillations were energy dependent, azide and non-metabolizable deoxyglucose were perfused into the chamber to deplete ATP levels [Moore and Blobel, 1992; Stenoien et al., 2001]. As shown in Figure 3D, centrosome movement

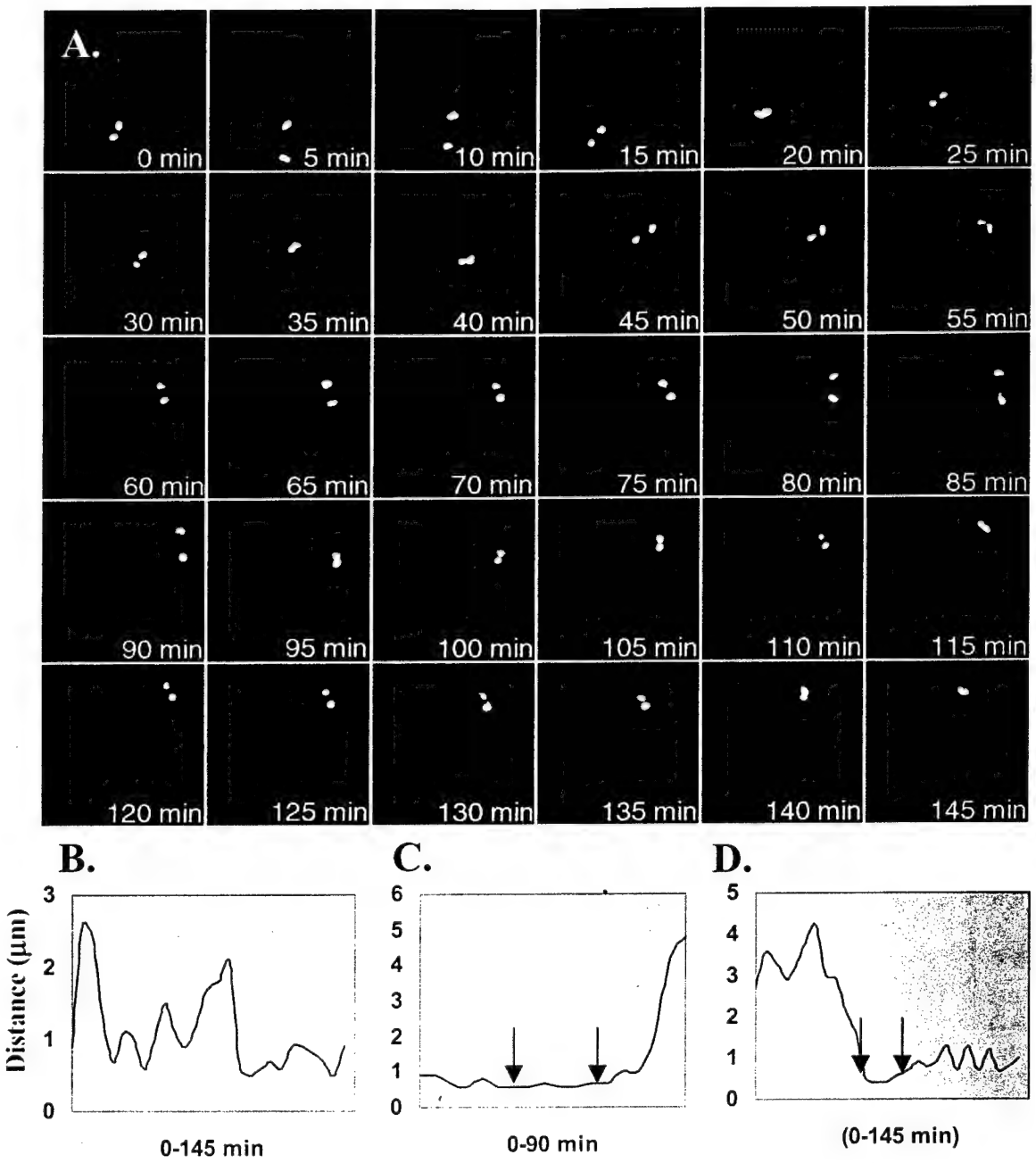

Fig. 3. Analysis of GFP-Aurora-A marked centrosomes during interphase. Live cell analysis was performed on GFP-Aurora-A expressing interphase cells. **A:** Shown is an example of a cell containing two centrosomes that undergo oscillatory movements relative to one another. **B:** The distance between centrosomes changes over time as shown by the graph. Depolimerization of microtubules by nocodazole treatment (**C**) or depletion of ATP levels (**D**) markedly reduces these oscillatory movements.

essentially stopped when ATP levels were depleted for ~20 min, but resumed when ATP was replenished by washing in normal media. While the oscillations resumed upon addition of normal media, they appeared attenuated suggesting that the recovery is incomplete.

Fluorescence recovery after photobleaching (FRAP) was employed to compare the relative mobility of GFP-Aurora-A, with GFP-labeled α-tubulin, γ-tubulin, and NuMA during interphase and mitosis. Although fixed cells studies suggest complete targeting to the centrosome, FRAP imaging reveals that GFP-Aurora-A moves rapidly in and out of the centrosome (Fig. 4A) and mitotic spindle (Fig. 4B) with recovery half-lives ($t_{1/2}$) on the order of seconds. The recovery curves plotted in

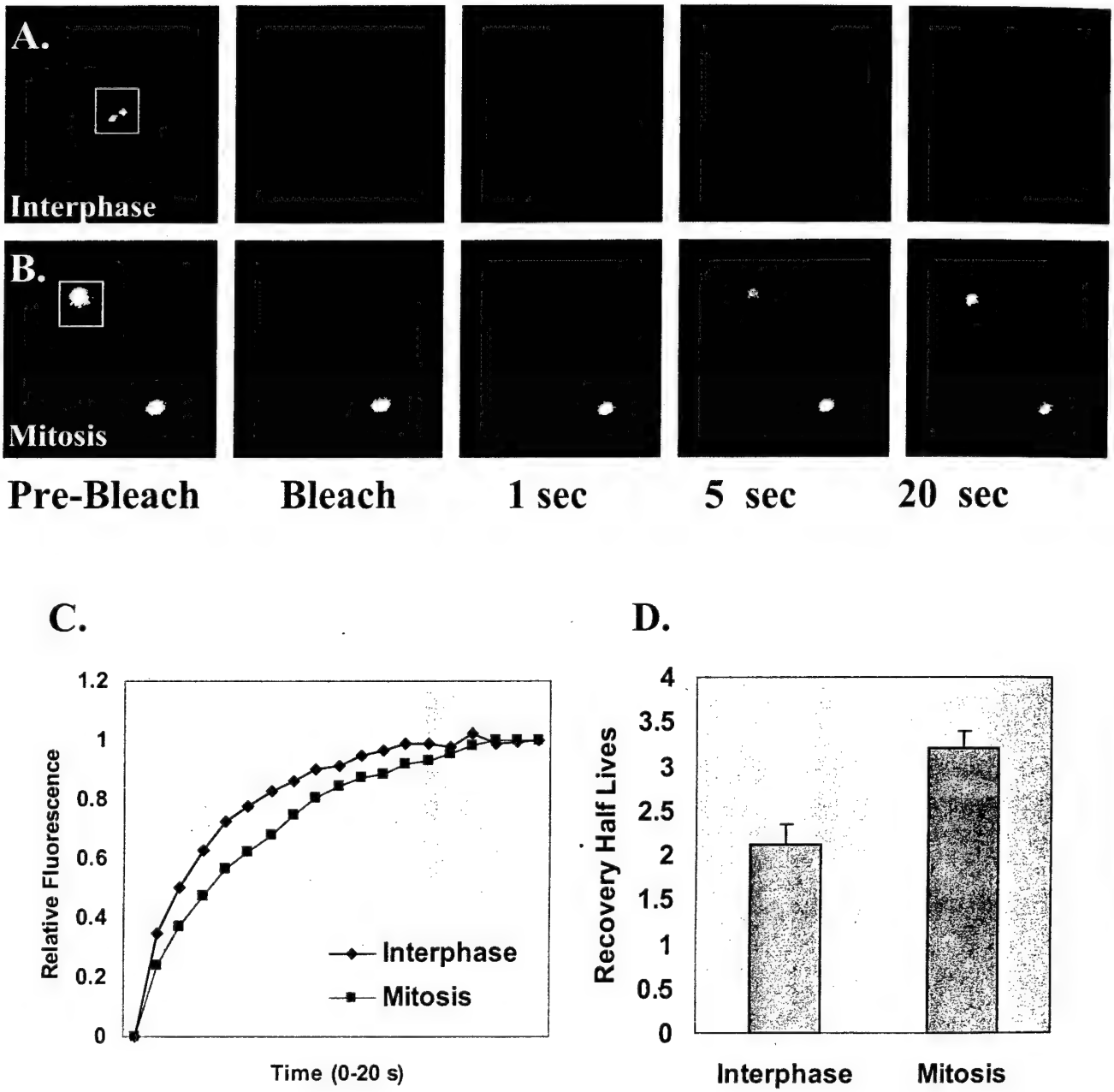

Fig. 4. GFP-Aurora-A is a dynamic component of the centrosome and mitotic spindle. FRAP analysis was performed on HeLa cells stably transfected with GFP-Aurora-A. Following a short photobleach in the region denoted by the box, GFP-Aurora-A recovers very rapidly at both the centrosome (**A**) and spindle (**B**). The recovery curves from 10 cells each are shown in **C** with the calculated $t_{1/2}$s shown in **D**. The $t_{1/2}$s of GFP-Aurora-A in the interphase centrosome and mitotic spindle are 2.1 ± 0.2 and 3.2 ± 0.2 sec, respectively.

Figure 4C show the dynamics are nearly identical in the centrosome and spindle. As shown in Figure 4D, the recovery half-live of GFP-Aurora-A was determined to be 2.1 ± 0.2 s (n = 10) in interphase centrosomes and 3.2 ± 0.2 s in mitotic spindles (n = 10). In cells containing two or more centrosomes (Fig. 5A), all centrosomes recovered at the same rate indicating that they are equivalent in their ability to recruit and/or exchange Aurora-A. Depletion of ATP levels (Fig. 5B and C) and nocodazole treatment (data not shown) had no noticeable effects on recovery times. Small variations in GFP-Aurora-A expression in the stable cell population

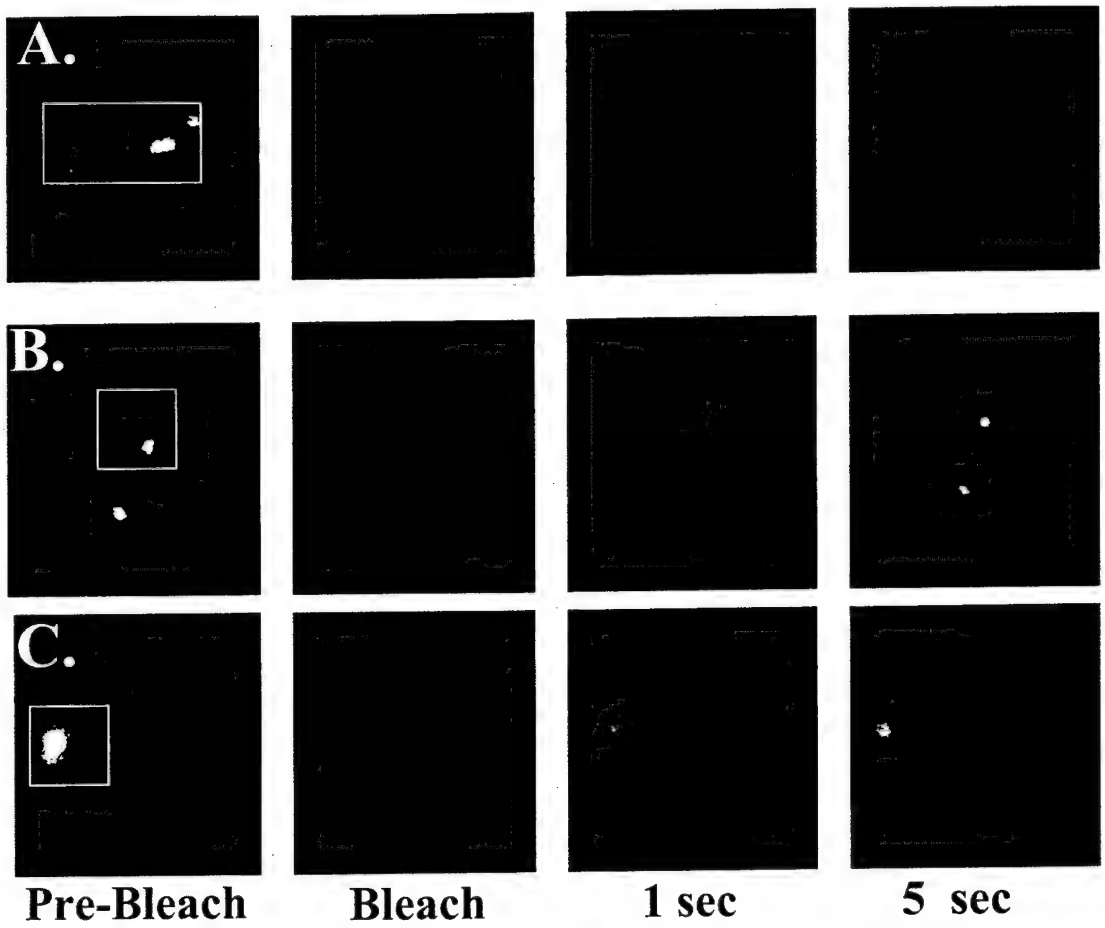

Fig. 5. Multiple centrosomes recover at the same rate and ATP depletion does not affect GFP-Aurora-A dynamics. **A:** When a cell containing multiple centrosomes marked by GFP-Aurora-A was photobleached, all centrosomes recovered at the same rate. To determine the requirements for ATP on Aurora-A dynamics, cells were incubated in glucose-free media supplemented with sodium azide and deoxyglucose for 15 min to deplete ATP levels. No difference in recovery times was observed in the presence of low ATP at both the centrosome (**B**) and spindle (**C**).

did not significantly affect recovery time suggesting that the recovery is concentration independent. Also, while the recovery occurs due to exchange of centrosomal GFP-Aurora-A with a freely diffusing GFP-Aurora-A pool, the recovery time at the centrosome can be thought of as a measure of the residence time at the centrosome rather than free diffusion through the centrosome that would occur on a much faster time scale.

In order to compare the relative mobility of other proteins located at the centrosome and/or spindle, stably transfected cells expressing GFP-γ-tubulin [Khodjakov and Rieder, 1999] and transiently transfected cells expressing GFP-α-tubulin or GFP-NuMA were subjected to FRAP analysis. In contrast to the rapid recovery of Aurora-A, both α and γ tubulins are relatively immobile showing little recovery over a period of one minute when centrosomal regions were bleached in interphase cells (Fig. 6A,B). GFP-γ-tubulin located at the spindle pole during mitosis (Fig. 6C) also exhibited much slower recovery than that observed with GFP-Aurora-A. The relatively slower recovery of GFP-γ-tubulin was previously reported by Khodjakov and Rieder [1999] who found that recovery to 50% of the starting fluorescence took 60 min in interphase centrosomes and 30 min in mitotic spindle poles. The nuclear mitotic apparatus protein (NuMA) exhibits intermediate mobility in both the interphase nucleus (Fig. 7A) and at the mitotic spindle (Fig. 7B) recovering completely within minutes. The average recovery curves are shown in Figure 7C. As shown in Figure 7D, the recovery half-life on GFP-NuMA is 23.4 ± 1.8 s (n = 8) in interphase cells and 30.7 ± 4.7 s in mitotic cells (n = 8). NuMA is known to redistribute from a diffuse, nuclear distribution to the mitotic spindle during mitosis and plays a significant role in anchoring spindle fibers to the mitotic poles [reviewed in He et al., 1995].

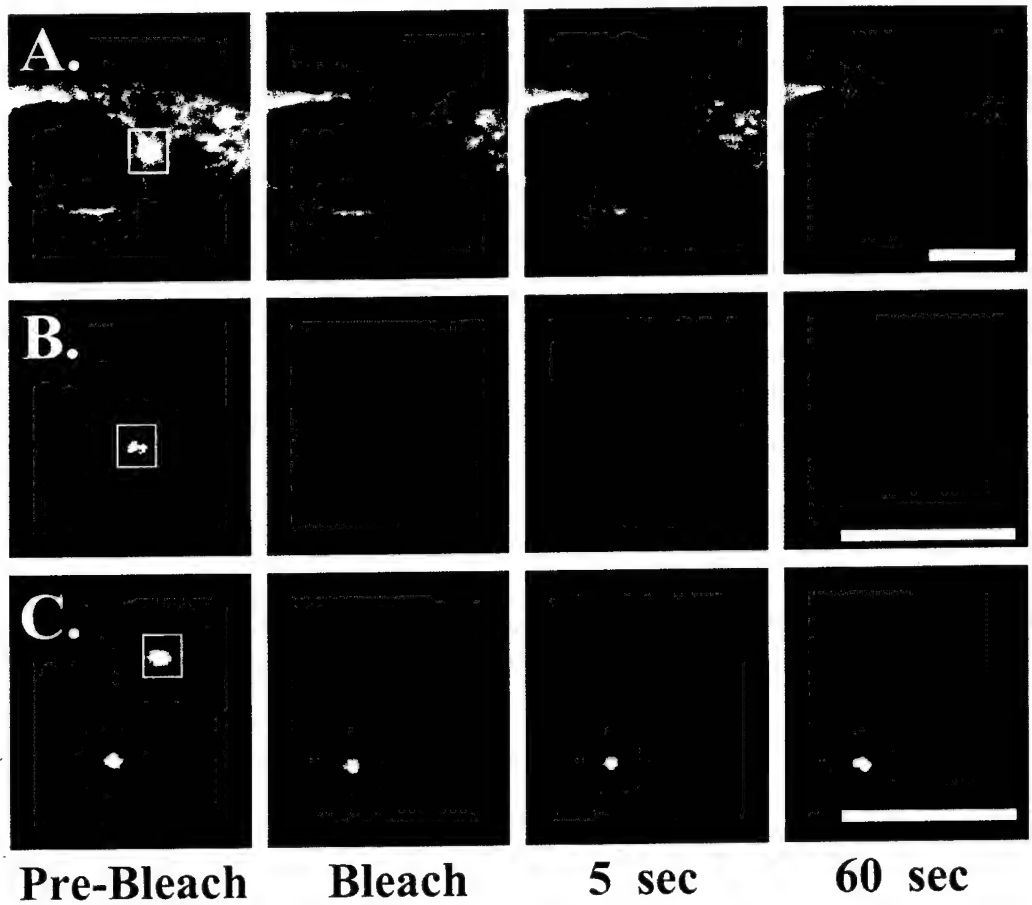

Fig. 6. Tubulins are stable components of the centrosome and mitotic spindle. FRAP analysis was performed on HeLa cells transfected with GFP-α-tubulin (**A**) or GFP-γ-tubulin (**B,C**). Little recovery is observed for both tubulins at the centrosome (A and B) or with gamma tubulin at the spindle pole over a period of 1 min (C).

To determine if specific domains of the Aurora-A are required for targeting to specific sites in the mitotic apparatus or if the molecular dynamics of Aurora-A are influenced by specific domains, mutational analyses were carried out as shown in Figure 8A. Constructs containing only amino acids 1–133 (DL1; Fig. 8B) shows no detectable centrosomal localization. This result is somewhat surprising since the corresponding region from the *Xenopus laevis* Aurora-A homologue has been reported to target to the centrosome [Giet and Prigent, 2001]. Our results indicate that centrosomal targeting of human Aurora-A requires at least amino acids 1–193 (DL2; Fig. 8C) for weak targeting and amino acids 1–310 (DL3; Fig. 8D) for strong centrosomal localization. The DL3 construct exhibits much slower recovery than the full-length Aurora-A (Fig. 8E). Deletion of the amino terminal 129 amino acids (DLN1) resulted in a protein that showed strong centrosomal localization and, interestingly, reduced photobleach recovery (Fig. 8F). A construct containing amino acids 130–310 (DLN1a) showed weak centrosomal localization (data not shown) similar to that observed with DL2 (Fig. 8C). Thus, our results indicate that the minimal centrosomal targeting sequence resides between amino acids 130–310 but sequences on the amino and carboxyl terminus are required for stronger centrosomal interactions. The reduced recovery times of DL3 and DLN1 suggest that domains in the amino and carboxyl terminus play a role in regulating the dynamics of Aurora-A localization to the centrosomes.

DISCUSSION

Since ectopic overexpression of Aurora-A has been shown to induce oncogenic transformation in cells [Bischoff et al., 1998, Zhou et al., 1998] and is implicated in chromosome instability, aneuploidy and tumorigenesis [Zhou et al., 1998, Sen et al., 2002), understanding its dynamic behavior during the cell cycle is crucial to characterizing the molecular control of this spindle

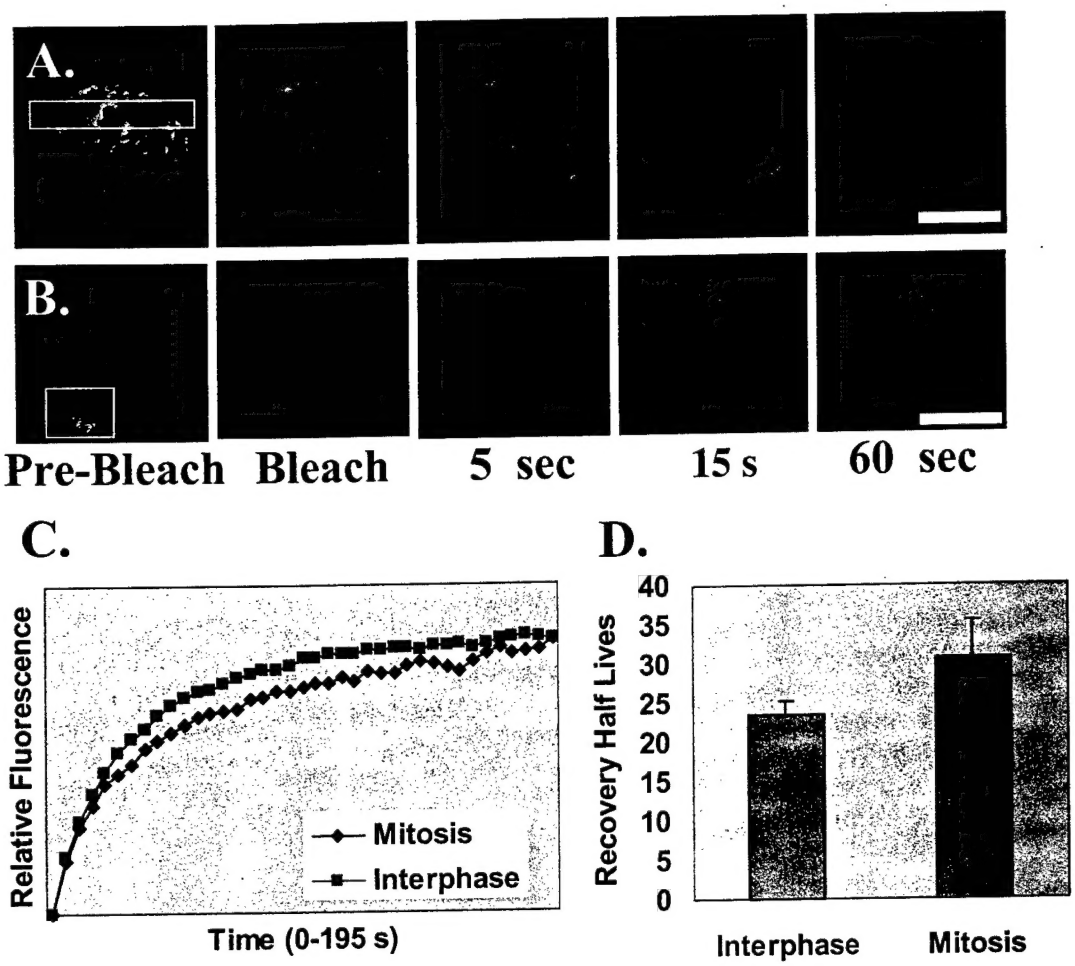

Fig. 7. NuMA shows intermediate mobility in the interphase nucleus and mitotic spindle. FRAP analysis was performed on interphase (**A**) and mitotic (**B**) HeLa cells transfected with GFP-NuMA. The average recovery profiles from a total of 8 cells each are plotted in **C** and show NuMA recovers completely within minutes in both the interphase nucleus and the mitotic spindle. The $t_{1/2}$s of NuMA are 23.4 ± 1.8 sec in interphase cells and 30.7 ± 4.7 sec in mitotic cells (**D**).

pole kinase, and developing strategies to counteract its deleterious effect on chromosome partitioning. In this study, we utilized live cell approaches to study the mechanisms by which Aurora-A interacts with interphase centrosomes and mitotic spindles. Our findings demonstrate that while Aurora-A accumulates on the centrosome and spindle throughout the cell cycle, the residence times of individual Aurora-A molecules at these sub-cellular locations are on the order of seconds, suggesting that a continuous dynamic exchange of Aurora-A at centrosomes and spindle occurs with its pool distributed in the cytoplasm. This finding contrasts with the relatively long residence times of structural proteins of the spindle including the tubulins and NuMA.

In contrast to a recent report showing the amino terminal non-catalytic domain of the *Xenopus laevis* Aurora-A homologue is sufficient for centrosomal localization [Giet and Prigen 2001], we find that this domain is not sufficient for targeting human Aurora-A and in fact is dispensable for targeting. Our results indicate that a region located between amino acids 130–310 is minimally required for Aurora-A targeting to the centrosomes. The differences in the targeting domains may reflect fundamental differences in the way in which Aurora-A targets the centrosome in different species. This could be accounted for by differences in the amino acid sequences in the two species. Notably, a stretch of 17 amino acids is present in the amino terminus of the Xenopus but not human Aurora-A that could contribute to targeting to the Xenopus centrosome. In addition, our results indicate that regions in the amino and carboxyl terminus strengthen centrosomal interactions suggesting that domains located throughout the human protein contribute to centrosomal binding.

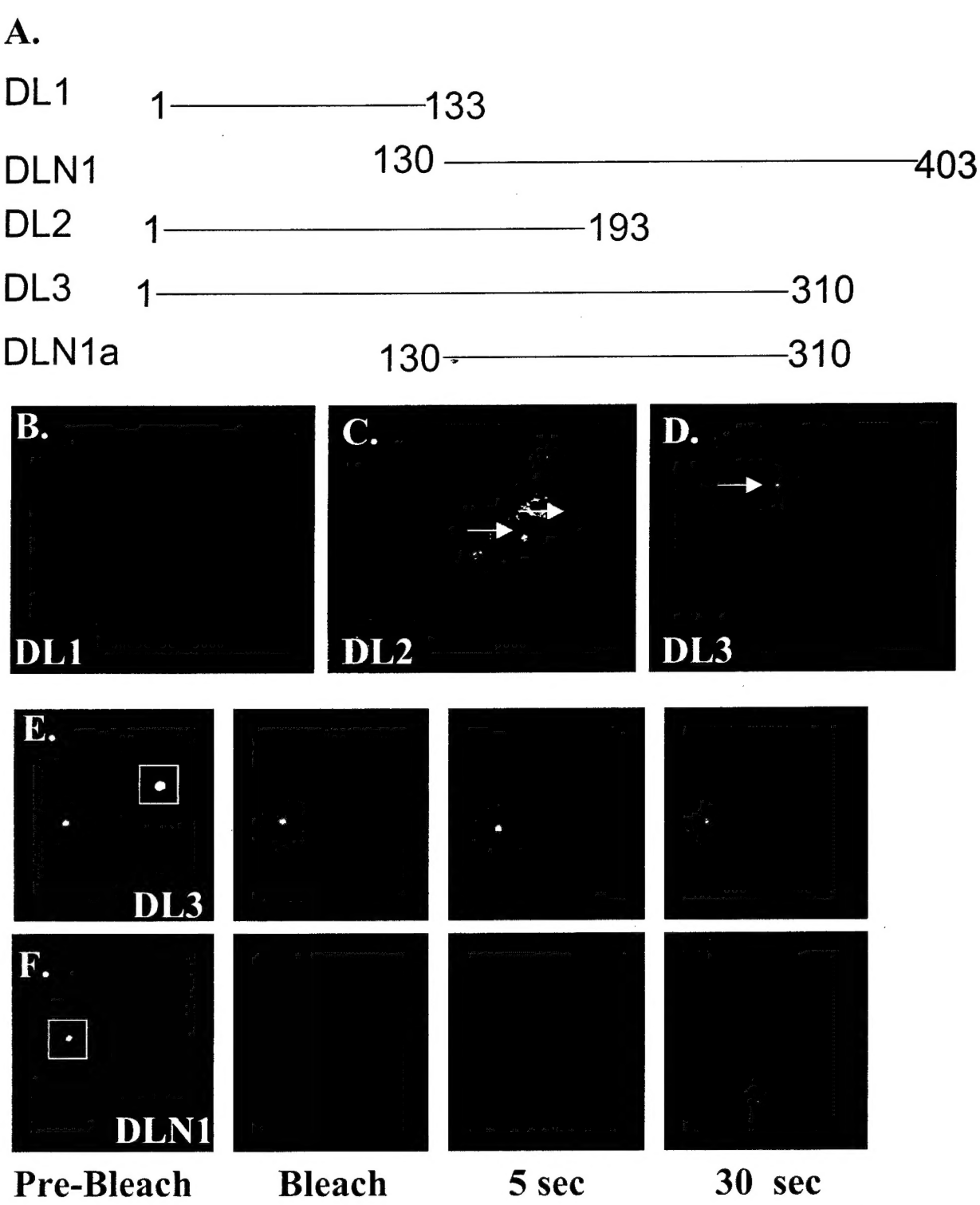

Fig. 8. Deletion analysis of centrosome targeting. **A:** Aurora-A deletions were generated as GFP fusions to analyze the effects on Aurora-A domains on centrosomal targeting. DL1 (1–133; **B**) did not target the centrosome. DL2 (aa 1–193; **C**) showed weak centrosome localization, and DL3 (aa 1–310; **D**) showed strong centrosome localization and reduced photobleach recovery (**E**). DLN1 (aa 130–403; **F**) behaved similar to DL3, showing strong centrosomal localization and decreased recovery after photobleach.

In addition to providing clues as to how Aurora-A targets the centrosome and spindle, GFP-Aurora-A has also proven to be a valuable tool to study centrosome and spindle dynamics in general. Earlier studies by Piel et al. [2000] used GFP-labeled centrin to document the movement of individual parent and daughter centrioles in living cells and provided the first evidence for a complex pattern of movement of daughter centrioles relative to mothers. In contrast to their study involving a probe that bound specifically to the distal lumen of the centriole, our probe, GFP- Aurora-A, excluded the centriole and bound to the pericentrosomal matix (data not shown). Thus, the pattern of movements observed herein involved the behavior of duplicated centrosomes, not individual centrioles. In contrast to centriole pairs where mother centrioles remained stationary while daughters moved about the cytoplasm in a complex pattern [Piel et al., 2000], centrosome pairs showed more coherent patterns of oscillatory movements with apparent collisions occurring between members of a single centrosome pair. In addition, both centrosomes appeared to undergo tumbling motions during the oscillations.

The observed dependence of microtubules and ATP on centrosome oscillations during interphase suggests that this phenomenon may be regulated by microtubule motor proteins. It is possible that these oscillations represent a competition between plus and minus MT-end directed motors. Interestingly, the tumbling motions of centrosomes also appeared to require microtubles and ATP and, therefore, this unusual motion, too, may be dependent on microtubule motor activity. The forces involved in tumbling motions remain unknown.

The recent use of FRAP to study the mobility of bioluminescent fusion proteins in live cells has shown that many proteins are much more dynamic than previously thought and forces a revision in the way we think about nuclear and cellular metabolism [Hager et al., 2000; Misteli, 2001]. These observations highlight the need to understand metabolic processes in the context of intact cells. FRAP analysis of centrosomal and spindle GFP-Aurora-A indicates that it is highly mobile (t1/2 ~2–3 sec), with recovery profile similar to documented observations of several proteins involved in nuclear metabolism [Phair and Misteli, 2000; Stenoien et al., 2001]. These findings suggest that proteins involved in various metabolic processes may need to reside at their functional sites for only a matter of seconds; indeed, reduced mobility of the estrogen receptor during certain conditions correlate well with transcriptional inactivation [Stenoien et al., 2001]. Structural proteins such as those forming the nuclear or cytoskeleton such as NuMA and tubulin are much less dynamic.

Collectively, our experiments contrast the relative cellular and molecular dynamics of Aurora-A with other cytoskeletal proteins that share overlapping micro-domains around the MTOC and spindle, and identify essential domains required for targeting and dynamics. The finding of greater molecular mobility of Aurora-A over tubulin and NuMA favors its dynamic relationship with centrosomes and spindles and supports a regulatory role in centrosome and spindle function.

ACKNOWLEDGMENTS

We thank Frank Herbert, Jeannie Zhong, Kavita Patel, Maureen Mancini, and Becky Moore for technical assistance and Betty Ledlie for editorial assistance in preparing the manuscript. This work was supported in part by grants NIH CA 41424, CA 64255 to B.R.B. S.S. was supported by NIH CA61979, NIH CA 89716, and DAMD 17-01-1-0302 from the US Department of Defense.

REFERENCES

Bischoff JR, Anderson L, Zhu Y, Mossie K, Ng L, Souza B, Schryver B, Flanagan P, Clairvoyant F, Ginther C, Chen CS, Novotny M., Slamon DJ, Plowman GD. 1998. A homologue of Drosophila aurora kinase is oncogenic and amplified in human colorectal cancers. EMBO J 17:3052–3065.

Brinkley BR, Stubblefield E. 1967. Ulatrastructure and interaction of the kinetochore and centriole in mitosis and meiosis. In: Prescott DM, Golstein L, McConkey E, editors. Advances in cell biology. New York, NY: Appleton-Century-Crofts. p 119–185.

Chan CS, Botstein D 1993. Isolation and characterization of chromosome-gain and increase-in-ploidy mutants in yeast. Genetics 135:677–691.

Chen S-S, Chang P-C, Cheng Y-W, Tang F-M, Lin Y-S. 2002. Suppression of the STK15 oncogenic activity requires a transactivation-independent p53 function. EMBO J 21:4491–4499.

Giet R, Prigent C. 2001. The non-catalytic domain of the *Xenopus laevis* aurora kinase localises the proteins to the centrosome. J Cell Sci 114:2095–2104.

Goepfert TM, Brinkley BR. 2000. The centrosome-associated aurora/Ipl-like kinase family, vol 49. In: Palazzo RE. Schatten G, editors. San Diego: Academic Press. p 331–342.

Goepfert TM, Adigun YE, Zhong L, Gay J, Medina D. Brinkley BR. 2002. Centrosome amplification and overexpression of aurora A are early events in rat mammary carcinogenesis. Cancer Res 62:4115–4122.

Hager GL, Lim CS, Elbi C, Baumann CT. 2000. Trafficking of nuclear receptors in living cells. J Steroid Biochem Mol Biol 74:249–254.

He D. Zeng C, Brinkley BR. 1995. Nuclear matrix proteins as structural and functional components of the mitotic apparatus, vol. 162B. In: Brezney R, Jeon KW, editors. San Diego: Academic Press. p 1–74.

Katayama H, Brinkley WR, Sen S. 2003. The Aurora kinases: role in cell transformation and tumorigenesis. In: Kumar R, editor. Cancer and metastisis reviews. The Netherlands: Kluwer Academic Publishers. Vol 22, p 451–464.

Khodjakov A, Rieder CL. 1999. The sudden recruitment of gamma-tubulin to the centrosome at the onset of mitosis and its dy-

namic exchange throughout the cell cycle, do not require microtubules. J Cell Biol 146:585–596.

Misteli T. 2001. Protein dynamics: implications for nuclear architecture and gene expression. Science 291:843–847.

Moore MS, Blobel G. 1992. The two steps of nuclear import, targeting to the nuclear envelope and translocation through the nuclear pore, require different cytosolic factors. Cell 69:939–950.

Mountain V, Compton DA. 2000. Dissecting the role of molecular motors in the mitotic spindle. Anat Rec 261:14–24.

Phair RD, Misteli T. 2000. High mobility of proteins in the mammalian cell nucleus. Nature 404:604–609.

Piel M, Meyer P, Khodjakov A, Rieder CL, Bornens M. 2000. The respective contributions of the mother and daughter centrioles to centrosome activity and behavior in vertebrate cells. J Cell Biol 149:317–330.

Sen S, Zhou H., Zhang R-D, Yoon DS, Vakar-Lopez F, Ito S, Jiang F, Johnston D, Grossman HB, Ruifrok AC, Katz RL, Brinkley W, Czerniak B. 2002. Amplification/overexpression of a motitic kinase gene in human bladder cancer. J Natl Cancer Inst 94: 1320–1328.

Stenoien DL. Patel K, Mancini MG, Dutertre M, Smith CL, O'Malley BW. Mancini MA. 2001. FRAP reveals that mobility of oestrogen receptor-alpha is ligand- and proteasome-dependent. Nat Cell Biol 3:15–23.

Zheng Y, Jung MK, Oakley BR. 1991. Gamma-tubulin is present in *Drosophila melanogaster* and *Homo sapiens* and is associated with the centrosome. Cell 65:817–823.

Zhou H. Huang J, Zhong L. Kuo W-L, Gray JW, Sahin A, Brinkley BR. Sen S. 1998. Tumor amplified kinase STK15/BTAK induces centrosome amplification, aneuploidy and transformation. Nat Genet 20:189–193.